APPENDIX B

Analysis of the Asbestos PCMe, Dust Lead Loading and Dust Dioxin Loading Data

Data analyzed in this report were extracted from the Residential database on September 10, 2003. A copy of the data set, with data necessary to protect the privacy of individual participants in the program redacted, is available from the EPA Region 2 Records Center.

B.1 SUMMARY OF DATA COLLECTED

B.1.1 Summary of TEM (PCMe) data

Table 3-1 summarizes the sample results for asbestos. The data described in this section and Section B.1.2 are results for asbestos phase contrast microscopy equivalent (PCMe) concentrations measured by transmission electron microscopy (TEM). A total of 28,702 sample results were available for asbestos by PCMe; 22,497 from residential units, and 6,205 from common areas within residential buildings (e.g., hallways, laundry rooms). Samples for PCMe analysis were collected from residential units that were tested only, as well as from residential units and common areas that were cleaned and tested. Results by PCMe were compared to the health-based benchmark of 0.0009 f/cc (fibers/cubic centimeter) to determine the status (i.e., exceeds or does not exceed benchmark) of the residential units/common areas.

The asbestos clearance criteria for the WTC Indoor Air Clean-up Program were based on long (i.e., $\geq$ 5 um) fiber counts. The use of a minimum fiber length of 5 μm for carcinogenic activity represents current scientific consensus and reflects the criteria in the EPA Integrated Risk Information System (IRIS) for attributing carcinogenic potency.

Phase Contrast Microscopy equivalence is a process to identify asbestos fibers by TEM analysis that would also be visible by PCM. The optical resolution of the phase contrast microscope is approximately 5 microns in length and 0.25 microns in width for fiber analysis. Historically,

most of the occupational studies available (and reviewed in IRIS), from which estimates of cancer potency of asbestos are derived, employed PCM analysis. Therefore, in cases where TEM is used for asbestos analysis, fiber counts need to be adjusted to estimate a PCMe.

The asbestos counting rules employed for the WTC Indoor Clean-up Program were designed to record PCMe fibers. Thus TEM analyses were performed, and fibers were then counted following AHERA (Asbestos Hazard Emergency Response Act) counting rules. Fibers ≥5 μm (AHERA also stipulates a minimum 5:1 aspect ratio) were distinguished from total (i.e., > 0.5 μm) fiber counts, although total fibers counts were also recorded. To maximize analytical capacity for a large sampling event, no minimum width requirement was employed. This may resulted in a modest over counting bias by not eliminating extremely thin fibers (i.e., <0.25 um) from the count. However, the potential bias attributed to this counting procedure would be protective of human health. Modification was made to AHERA (by obtaining larger samples volumes) in order to achieve the lower detection limits required by the use of a risk-based clearance criteria.

B.1.2 Summary of TEM data.

Table3-2 lists the types of asbestos that were detected by TEM in the airborne asbestos samples from residences and common areas. Asbestos was detected in approximately 4% of the available TEM samples. Chrysotile asbestos was the detected in approximately 92% of the samples included in this subset of the data; amosite was detected in approximately 3%. Other forms of asbestos that were detected include actinolite, anthophyllite, tremolite, and crocidolite.

B.1.3 Summary of Wipe data

B.1.3.1 Lead and dioxin wipe data

This section of the report describes lead and dioxin dust wipe data that were collected from 263 residences that were located in 157 buildings. Wipe data that were used to assess efficacy of the cleanup program are discussed in Section B.4

B.1.3.1.1 Lead Wipe Data

The database contained 1,540 wipe samples for dust lead loading that were collected from 263 residences, located in 157 buildings. Summary statistics for the data are provided in Table 3-3. Samples that were below the detection limit of 1.86 $\mu g/ft^2$ were set equal to the detection limit. Review of existing environmental standards/regulations identified an applicable and relevant standard to set a health-based benchmark for lead in interior dust. The Residential Lead-Based Paint Hazard Reduction Act (Title X) Final Rule (40 CFR, Part 745, 1/5/01) established uniform national standards for lead in interior dust. Thus, both EPA and the United States Department of Housing and Urban Development (HUD) have set a dust standard for lead of 40 $\mu g/ft^2$ for floors (including carpeted floors), and 250 $\mu g/ft^2$ for interior window sills. To support the development of a dust standard, EPA performed an analysis of the Rochester Lead-in-Dust Study (HUD, 1995). At 40 $\mu g/ft^2$, a multimedia analysis shows a 5.3% probability that a child's blood lead level would exceed 10 μg/dL. Thus, this standard meets the criteria established by EPA (i.e., 95% probability to be below 10 μg/dL) (EPA, 1994) for managing environmental lead hazards. However, an additional increment of protectiveness was added by setting the health-based benchmark for lead in settled dust at the more stringent HUD screening level of 25 $\mu g/ft^2$. Approximately 9% of all lead wipe samples (i.e., *test only* and *clean and test*) were above the HUD screening level of 25 $\mu g/ft^2$ (Table 3-3); approximately 14% of the pre-cleanup samples exceeded the HUD screening level , while approximately 3% of the post-cleanup samples exceeded the screening level (Tables 3-4 and 3-5). Approximately 6% of the samples were above the HUD benchmark of 40 $\mu g/ft^2$ (Table 3-3).

B.1.3.1.2 Dioxin Wipe Data

The database contained 1,535 wipe samples for dust dioxin loading that were collected from 263 residences, located in 157 buildings. Summary statistics for the data are provided in Table 3-6. The dioxin results were modified using a toxicity equivalency quotient (TEQ) that takes into account the toxicity differences between 17 congener groups**.** The results are reported in 2,3,7,8-tetrachlorodibenzo-p-dioxin (TCDD) toxicity equivalents. The TEQ values reported in Table 3-6 represent the estimated maximum potential concentration (EMPC). The TEQ EMPC value used data that indicated the presence of a congener above zero mg/m^2 even if the sample did not meet

all of the QA/QC reporting level criteria. This value represents the highest potential concentration of dioxin that may be present. At least one of the 17 congeners were detected in 1,136 of the samples; the remaining 399 samples were reported as below the detection limit for each congener. Only 8 of the 1,535 (approximately 0.5%) of the combined samples (i.e., *test only* and *clean and test*; Table 3-6) exceeded the health-based benchmark for residential dust dioxin loading of 2 ng/m2 (Table 3-6).

B.1.3.2 Wipe Data for Other Metals

Statistics for the 21 metals, and the reduction in the average dust loading rates for each, are provided in Table 3-7. The data are grouped into three categories in Table 3-7: samples collected from residences and common areas that were cleaned and tested (*clean and test samples*), samples that were collected from residences that were tested only (*test only samples*), and the combination of these two categories (*all samples*).

The database contained 1,517 results for mercury, and 1,544 results for all of the other metals. The rate of detection (based on all samples) varies widely from 0, for beryllium and thallium, to 100%, for calcium, copper, iron, magnesium, potassium and zinc. Eight of the 21 metals had detection rates of less than or equal to 5%; 4 had detection rates between 6 and 60%. Results for each metal were compared against risk-based screening levels (Table 3-8). Very few exceedances of the risk-based screening values were measured for any of the metals. The screening value of 627 $\mu g/m^2$, for antimony, was exceeded in 2 pre-cleanup samples (0.1% of all samples); the maximum measured value was 1,180 $\mu g/m^2$. The screening value of 157 $\mu g/m^2$ for mercury was exceeded in six samples (0.4% of all samples).

B.2 EFFICACY OF THE DUST CLEANUP EFFORT

B.2.1 Reductions in the Rate of Asbestos PCMe Exceedances

The efficacy of the asbestos cleanup effort was assessed using PCMe exceedances for *clean and test* data. One measure of effectiveness is the overall rate of exceedances, which equals the number of exceedances divided by the total number of samples that were collected (i.e., rate on a

sample basis). The overall exceedance rate on a sample-basis for the WTC cleanup program was approximately 0.00418, or 0.42%.

An alternative measure of efficacy is the number of times a residence or a common area within a building (e.g., hallway, stairwell, laundry) had to be recleaned to achieve the clearance criteria of 0.0009 f/cc. The cleanup effort was effective in achieving the clearance criteria for PCMe approximately 99% of the time in residential units and common areas. The PCMe clearance criterion was not achieved in 35 out of 3,387 (1.03%) residences, and in 11 out of 785 common areas (1.40%) after the first cleaning. The probability of achieving the clearance on the second attempt in residential units that did not achieve clearance after the first cleaning approached 1 (>0.999; 2 out of the 25 residences that were recleaned did not achieve clearance after the second cleaning - 10 residents elected not to have their residences recleaned, or were unresponsive). The cleaning methods used were effective in reducing asbestos concentrations in residential air.

A *modified aggressive* sampling procedure was used in most of the apartments (EPA, 2003a). The modified-aggressive sampling procedure was adapted from the aggressive sampling procedure described in AHERA. The aggressive sampling procedure had a tendency to overload the sampling filter with dust, preventing the samples from being analyzed by the laboratory (EPA, 2003a). The modified aggressive sampling is thought to be more representative of typical household activity patterns (EPA, 2003a). The rate of exceedance varied between the two sampling procedures. On a sample basis, the exceedances rates in *test only* residences were 0.50 and 0.49% for the aggressive and modified aggressive sampling procedures, respectively; the exceedances rates for the *clean and test* residences were 3.4 and 0.20% for the aggressive and modified aggressive sampling procedures, respectively. The test only exceedances rates were not significantly different by Fisher's exact test ($p>0.99$); the *clean and test* exceedances rates were statistically significant by Fisher's exact test ($p<0.01$). On a residence-basis (i.e., one or more sample result from the residence equal or exceeded the benchmark for asbestos), the exceedances rates in *test only* residences were 3.0 and 1.1% for the aggressive and modified aggressive sampling procedures, respectively; the exceedances rates for the *clean and test* residences were 6.4 and 0.64% for the aggressive and modified aggressive sampling procedures, respectively. The *test only* exceedances rates were not significantly different by Fisher's exact test ($p>0.34$); the *clean and test* exceedances rates were statistically significant by Fisher's exact test ($p<0.01$).

B.2.2 Reductions in dust lead loadings

The indoor environment is considered to be a complex and dynamic system that is influenced by many interacting factors (physical, chemical, thermodynamic conditions, human activity, building design, building materials, HVAC system, etc.) Therefore, it is not uncommon to find variability in the amount of contaminants in settled dust within a building, and certainly from one building to the next. In addition to WTC proximity, the large CV is also likely due to the wide range of diversity in the housing stock, contents of the residences and common areas, and preexisting conditions, or previous activity, at these sites.

To assess the effectiveness of the cleanup program, the wipe data were divided into two groups: samples that were collected before the apartments were cleaned (*pre-cleanup)*, and samples that were collected after the apartments were cleaned (*post-cleanup)*. Pre-cleanup lead wipe samples and post-cleanup samples were collected from 214 apartments, located in 145 buildings. Samples that were below the detection limit of 1.86 μg/ft^2 were set equal to the detection limit. Table 3-4 provides statistics for the pre-cleanup and post-cleanup lead wipe data; a more complete set of statistics is provided in Appendix A, Table A-1. On average, three pre-cleanup and three post-cleanup wipe samples were collected from each apartment (see Section 2.2 for an overview of the cleanup program).

The data are highly positively skewed with a very large coefficient of variation (CV). The high positive skewness indicates that a few lead wipe samples contained much higher levels of lead than the majority of the samples (Figure B-1). The large CV indicates the data are highly variable; i.e., the lead wipe samples indicate the dust lead loadings vary over a wide range of values. One factor that is a likely contributor to variability in lead wipe sampling results is the presence of lead-based paint in older (i.e., pre 1950) housing. This factor is exemplified in the case of the two highest recorded lead wipe samples in the data set. These two samples were pre- (6,790 μg/ft2) and post-cleaning (7,250 μg/ft2) wipes obtained from the top of a storage chest. The lead loading measured in the two other pre-cleanup lead wipe samples collected from this residence was 3.57 and 91.8 μg/ft^2, and the lead loading in the two other post-cleanup samples was 7.41 and 7.56 μg/ft^2. The extremely high lead loads in these two matched samples prompted additional investigation which determined that the chest surface was remarkable for flaking paint. A paint chip sample was analyzed and contained 14% (140,000 μg/kg) lead, thus, providing a

plausible explanation for the aforementioned sampling results. Table 3-5 provides statistics for the pre-cleanup and post-cleanup lead wipe data with the above two values removed, as

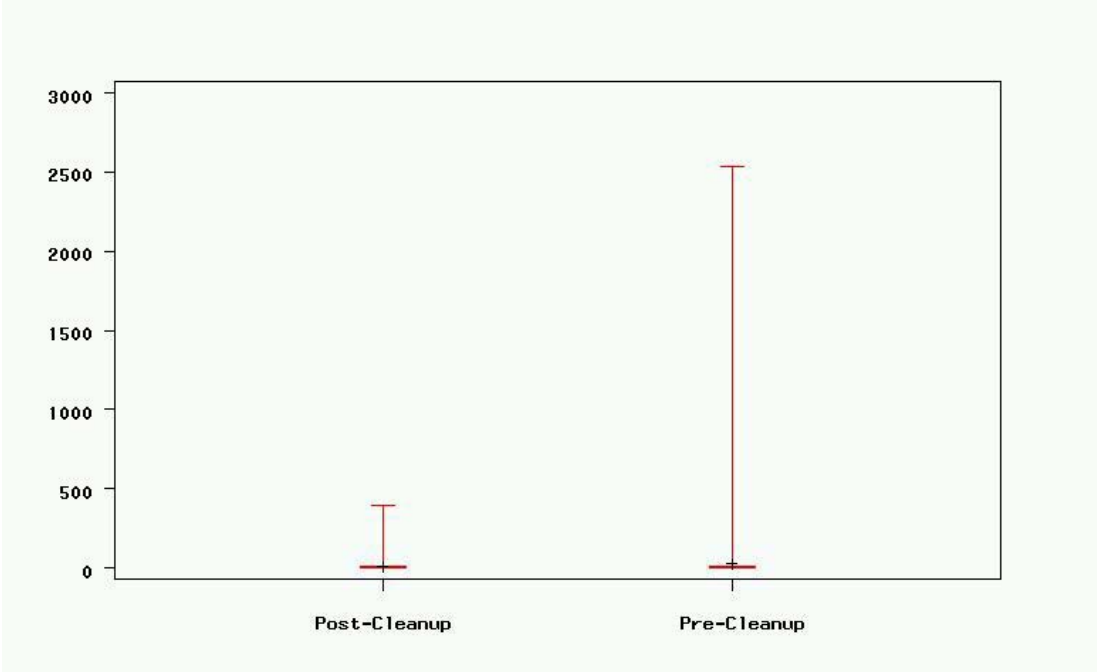

mple type.
ngs exhibit
onsists of
x is drawn
25th %; the
ndicated
oincide.
m value;
xtreme
he box
greatly
data

outliers; a more complete set of statistics is provided in Appendix A, Table A-1a. Although the above two outliers were excluded from the remainder of the analyses of the lead wipe data, their inclusion would not have changed the results of the statistical tests that are described later in this section.

The high CV and skewness often mask differences between subsets of the data; e.g., between pre-cleanup and post-cleanup dust lead levels. The issue of high CV and skewness are closely related to the issue of normality. Many statistical methods for comparing two or more sets or subsets of data are based on an assumption that the data are derived from a normal distribution. As shown in Figures B-2 and B-3, a normal distribution is a bell-shaped curve that is symmetric about the mean (i.e., skewness=0). One method of reducing the skewness and CV, thereby improving the fit of a normal distribution to the data, is to take the logarithms of the data. Log-transformation of the data reduced the skewness to 1.17 and 0.71 for the pre-cleanup and post-cleanup data, respectively, and the CV to 0.57 and 0.48, respectively. Likewise, tests for normality[1] indicate the log-transformation improved the fit of a normal distribution to the pre-cleanup and post-cleanup data (S-W statistic increased to 0.90 and 0.89, respectively) however, the log-transformed data continue to display substantial departures from normality ($p<0.0001$ for both subsets).

The cleanup program reduced the overall number of exceedances from 92 (13.5 % of samples) to 20 (3.0% of samples). The mean and median of the combined post-cleanup data are less than the pre-cleanup data (Table 3-5).

One approach to assessing the effectiveness of the cleanup program would be to compare the distribution of the 680 pre-cleanup samples to the 673 post-cleanup samples, taking into account various factors that effect lead loading in residential areas (e.g., the amount and condition of lead-based paint, the amount of carpeted floors, the amount of upholstered furniture). This approach would provide the ability to estimate the effects of these various factors on the effectiveness of the cleanup program; however, data for these various factors are not readily available for the cleanup program.

---

[1] The following tests for normality were performed in each case: Anderson Darling, Cramer-von Mises, Kolmogorov-Smirnoff, and Shapiro-Wilk.

An alternative to the above approach would be to calculate the difference between the mean pre-cleanup and mean post-cleanup lead wipe loadings for each of the 214 residences, and comparing the 214 differences. The advantage of analyzing the differences between pre-cleanup and post-cleanup loadings

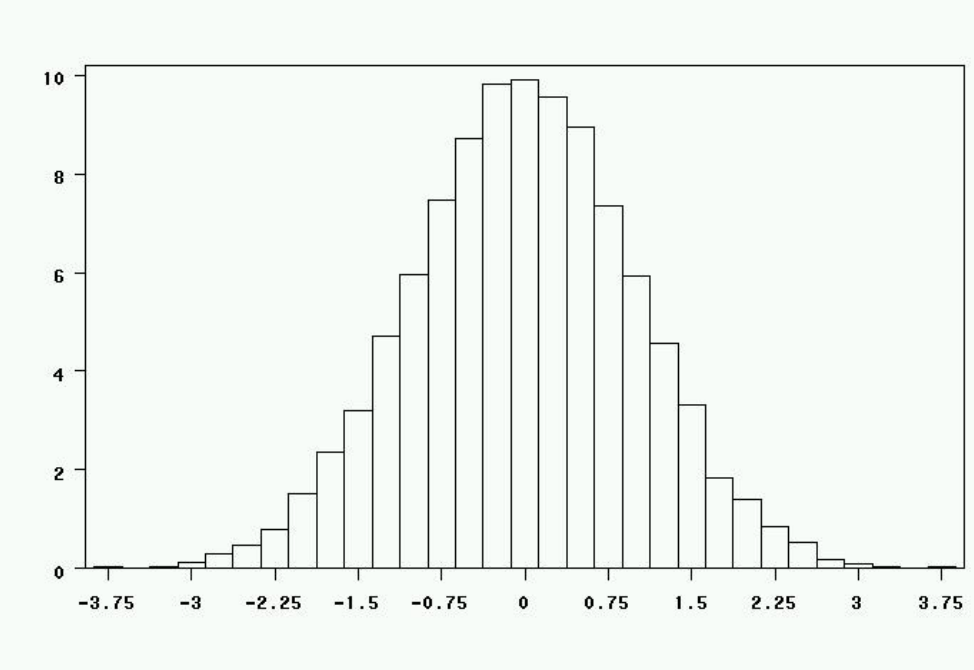

Figure B-2. Histogram for 10,000 randomly generated samples from a standard normal distribution. The value of the sample is shown on the x-axis, the y-axis shows the percent of the 10,000 samples that have the value indicated on the x-axis. For example, approximately 10% of the 10,000 samples have a value of approximately 0. The normal distribution is a bell-shaped curve that is symmetric about the mean, which equals 0 for the standard normal distribution. For any normal distribution, approximately 66% of the observations occur within a distance of 1 standard deviation of the mean; approximately 95% occur within a distance of 2 standard deviations of the mean. For example, approximately 66% of the 10,000 simulated values fall within the interval bounded by -1 and +1 and, approximately 95% of the values fall within the interval bounded by -2 and +2.

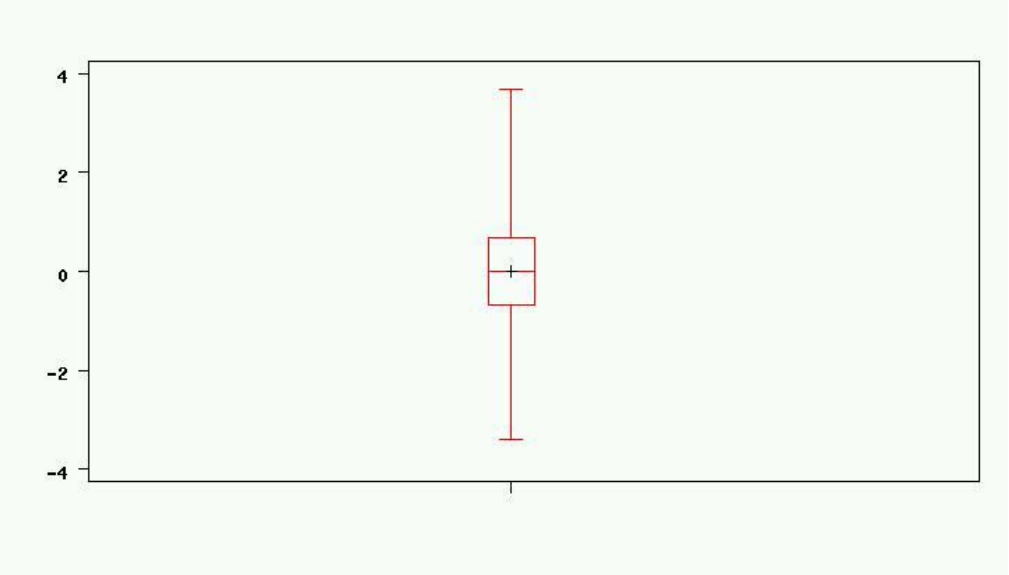

Figure B-3. Boxplot for 10,000 randomly generated samples from a standard normal distribution. The values of the samples (i.e., z-values or standard normal deviates) are shown on the y-axis. The boxplot is another method of illustrating the distribution of a sample. As shown above, the boxplot for a normal distribution is symmetric about the mean/median. The median (indicated by horizontal line that is located within the box) and mean (indicated by black '+') of a normal distribution are equal, and located at the center of the box. The 25th percentile of the distribution (indicated by the bottom of the box) and the 75th percentile (indicated by the top of the box) are equidistant from the median/mean; the extreme values (indicated by the short horizontal lines at the end of the vertical lines that emanate from the box) as are also approximately equidistant from the median/mean. The skewness of a normal distribution equals zero; a positively skewed population is characterized by a few observations that are much larger than the rest of the observation; see Figure 3-1 for an example of extreme positive skewness.

on a residence-by-residence basis is that it takes into consideration the multiple factors (e.g., age of buildings) that effect the dust lead loadings in an apartment, without the need to explicitly incorporate these factors in the analyses. Statistical comparisons between the pre-cleanup and post-cleanup dust lead loadings using the second approach will tend to be more powerful than those made using the first approach when multiple factors affect the dust lead loading[2]. Therefore, the second approach was adopted for this analysis.

Table B-1 presents statistics on the average pre-cleanup and post-cleanup dust lead loadings, on a residence-by-residence basis, and the reduction in the average dust lead loading for the 214 cleaned residences. A more complete set of statistics for lead wipe reductions is provided in Appendix A, Table A-2. The dust lead loadings shown in Table B-1 are average loadings for each residence that were estimated with approximately three pre- and three post-cleanup samples collected from each residence. The distribution of the reductions is positively skewed with high variance (Figure B-4). Tests for normality indicate the normal distribution provides a poor fit to the data. A log-normal transformation of the data fails to substantially improve normality (S-W=0.37, $p<0.0001$). The evaluation to determine the efficacy of the cleanup program, presented below, considers the high variance, skewness and deviation from normality exhibited by the data.

On average, the cleanup program reduced the average dust lead loading in each residence by approximately 16 $\mu g/ft^2$ (95% confidence interval [CI][3], 10.0, 29.4%). The reduction in the mean dust lead loading was found to be statistically significant by the t-test (t=3.64, p=0.0003). The t-test assumes the differences are normally distributed, which is a questionable assumption for this data (Table B-1). As a check on the apparent violation of the normality assumption, the significance of the reduction in dust lead loadings was also tested using the nonparametric sign test. The sign test assumes only that

---

[2] The addition of factors in the analyses decreases the degrees of freedom that are available to compare the pre-cleanup dust lead loadings with the post-cleanup loadings.

[3] Confidence interval was determined by bootstrapping, using the bias-corrected accelerated (BCa) method (Efron and Tibshirani, 1993). The BC bootstrap method does not rely on an assumption of normality for the distribution of the mean of the reduction in dust lead loadings, and is therefore preferred over the typical method (i.e., using the t-distribution) for this data.

Table B-1. Reduction in Average Lead Wipe Loadings (Pre- and Post-cleanup) (µg/ft^2).

Statistics for average pre-cleanup and post-cleanup residential dust lead loading measured by wipe samples are shown, and statistics for the reduction in the average dust lead loading. The average dust lead loadings and the reduction in the averages, continue to display substantial departures from normality; a log-transformation of the data fails to improve the fit of a normal distribution to the data (S-W statistic for reductions=0.37 , $p<0.0001$; pre-cleanup averages: S-W statistic=0.95, $p<0.0001$; post-cleanup averages: S-W statistic=0.92). Outliers were removed from the dataset (see Section 3.4.1 for details).

Statistic	Reduction in Average Lead Wipe Loading	Average Pre-cleanup Lead Wipe Loading	Average Post-cleanup Lead Wipe Loading
n	214	214	214
Mean	16.21	24.40	8.19
Standard deviation	65.16	66.34	17.10
Skewness	7.23	7.73	12.17
CV[a]	4.02	2.727	2.096
Var	4245.98	4401.40	292.29
Maximum	708.21	748.95	241.67
Median	1.77	8.66	6.79
Minimum	-163.27	1.86	1.86
S-W Statistic[b]	0.33	0.15	0.22
Prob Normal[c]	<0.0001	<0.0001	<0.0001

[a]CV=coefficient of variation=standard deviation/mean
[b]S-W Statistic: Shapiro-Wilk statistic
[c]Prob Normal: probability the data are from a normal distribution by Shapiro-Wilk test.

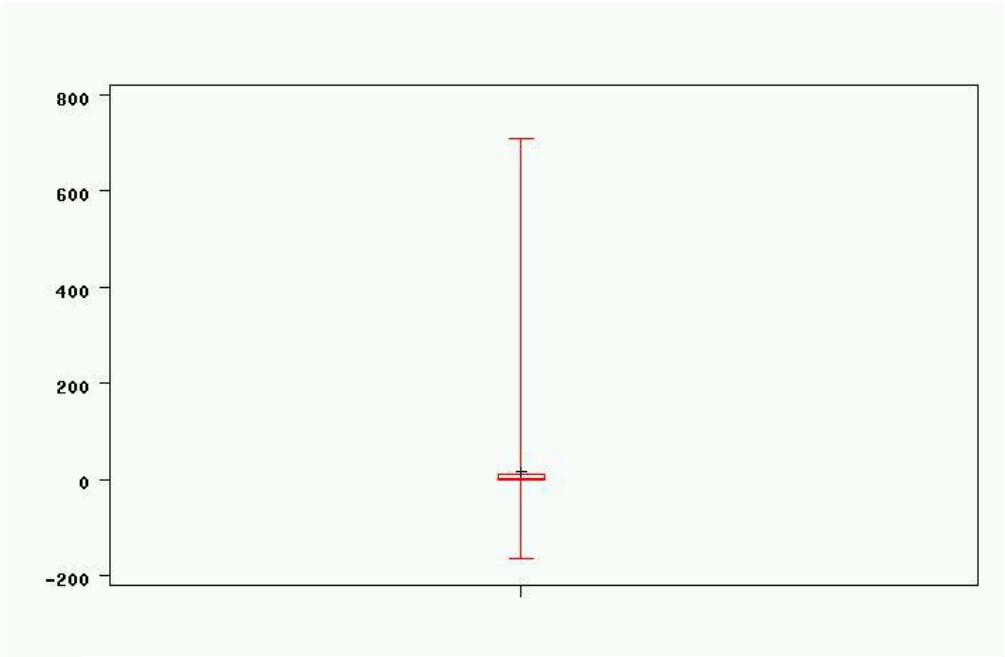

Figure B-4. Boxplot for the reduction in residential average dust lead loading ($\mu g/ft^2$). The short 'box' indicates the majority of the reductions occur within a very short range of values; 50% of the reductions are between 0 and 9.50 $\mu g/ft^2$.

the differences between the pre-cleanup and post-cleanup means are independent random variables[4]. The sign test considers only the direction of the difference (i.e., positive or negative), not the magnitude of the differences, which removes the effects of the extreme measurements (which produce the positive skewness) on the test results. The sign test also indicated the reduction in the dust lead loadings were significant (M=53.5, $p<0.0001$).

The effect of cleaning can also be expressed as a percent decrease in the dust lead loading (Equation B-13). The mean percent reduction in dust lead loading was 20.4% (95% CI[3], 8.8, 27.9%). The data set included two extreme negative percent decreases; an increase in mean dust lead loading of 485% that corresponded to an increase from a pre-cleanup mean loading of 4.9 μg/ft^2 to a post-cleanup loading of 27.1 for a 22nd floor residence, and an increase from 4.4 to 25.9 μg/ft^2 for a 5th floor residence. After these observations were removed from the data, the mean percent reduction in dust lead loading was 25.0% (95% CI, 17.7, 31.3%).

$$Percent\ decrease = 100 \cdot \frac{\left(\bar{x}_{pre} - \bar{x}_{post}\right)}{\bar{x}_{pre}} \qquad \text{Equation B-13}$$

Where,

$\bar{x}_{pre}$ = *average pre-cleanup dust lead loading*

$\bar{x}_{pre}$ = *average post-cleanup dust lead loading*

Another method for analyzing the effectiveness of the cleanup program in reducing dust lead loadings is to determine the rate (i.e., proportion of residences) at which the average dust lead loadings were reduced by the cleanup. In 9 of the residences, all of the average pre- and post-cleanup dust lead loading measurements were less than the detection limit. Of the remaining 205 residences, the post-cleanup average dust lead loading was greater than the pre-cleanup average in 49 residences, and lower in the other 156 residences, yielding a rate of reduction of approximately 76%. The sign test discussed in the previous paragraph is based on the number of

---

[4] This assumption is also not strictly valid because random sampling methods were not used to select which residences were cleaned (it was a voluntary program) and random sampling methods were not used to select the subset of the cleaned residences where dust wipe samples were collected.

reductions (i.e., not the magnitude of the reductions) and, therefore, provides a test for the statistical significance for the rate of reduction (i.e., the number of reductions / the number of *cleaned and tested* residences). Therefore, the sign test indicates that the rate at which the cleanup program lowered the average residential dust lead loading is statistically significant ($M=53.5$, $p<0.0001$).

B.2.2.1 Reductions in dust lead loadings in residences with pre-cleanup levels greater than the health-based benchmarks for lead loading

The effectiveness of the cleanup program at reducing dust lead loading in the 36 residences that had pre-cleanup dust lead loadings greater than the HUD screening level of 25 $\mu g/ft^2$ was assessed. Table B-2 provides statistics for dust lead loading for these residences; a more complete set of statistics is provided in Appendix A, Table A-3. The dust lead loadings shown in Table B-2 are average loadings for each residence that were estimated with approximately three pre- and three post-cleanup samples collected from each residence. As expected, the distributions of the average pre-cleanup, post-cleanup and dust lead loading reductions for this subset of the data are less skewed and have lower CVs than the distribution of the lead loadings for all 214 sampled apartments. The log-transformation of the reductions in the average loading does not substantially improve normality (S-W statistic=0.71, $p<0.0001$).

Thirty-six residences had pre-cleanup average dust lead loadings greater than the HUD screening of 25 $\mu g/ft^2$. The cleanup program reduced the average dust lead loading in the residences with average pre-cleanup loadings above the HUD screening level by approximately 85 $\mu g/ft^2$ (95% CI,[3] 71.2, 173.6%). The reduction in the average dust lead loading was found to be statistically significant (t-test, $t=3.61$, $p=0.0009$; sign test, $M=17$, $p<0.0001$).

The cleanup program was successful in reducing average dust lead loading in 31 of the 36 residences to below the 25 $\mu g/ft^2$ HUD screening level, a success rate of approximately 86%. In four other residences, the average post-cleanup dust lead loading was substantially reduced, but remained above 25 $\mu g/ft^2$; from 749.0 to 40.7, 149.3 to 28.8; 120.9 to 39.2; 83.2 to 40.7; and 61.6 to 31.7 $\mu g/ft^2$. The post-cleanup average increased from 78 to 242 $\mu g/ft^2$ in one residence. In three cases, a residence with a pre-cleanup average dust lead loading less than the screening level had a post-cleanup average that exceeded the screening level. The increases in post-cleanup

average dust lead loadings could reflect sampling variability or site-specific factors that can not be assessed with data that are currently available.

Table B-2. Statistics on Reduction in Average Lead Wipe Loadings (Pre- and Post-cleanup) (µg/ft^2) in Residences with Pre-cleanup Greater Than the Health-based Benchmark of 25 ug/ft^2.

The average dust lead loadings and the reduction in the averages show less variation and are less skewed than the complete distribution of average residential dust lead loadings. A log-transformation of the averages slightly improves the fit of a normal distribution to the data (S-W statistic for reductions=0.71, p<0.0001; pre-cleanup averages: S-W statistic=0.89, p<0.0001; post-cleanup averages: S-W statistic=0.88, p<0.0001); however, significant departures from the normal distribution model remain. Outliers were removed from the dataset (see Section 3.4.1 for details).

Statistic	Reduction in Average Lead Wipe Loading	Average Pre-cleanup Lead Wipe Loading	Average Post-cleanup Lead Wipe Loading
n	36	36	36
Mean	84.84	102.12	17.28
Standard deviation	140.85	138.37	39.62
Skewness	2.90	3.47	5.49
CV[a]	166.01	135.50	229.28
Var	19838.34	19147.47	1569.75
Maximum	708.21	748.95	241.67
Median	38.82	48.52	8.08
Minimum	-163.27	25.86	1.86
S-W Statistic[b]	0.64	0.56	0.32
Prob Normal[c]	<0.0001	<0.0001	<0.0001

[a]CV=coefficient of variation=standard deviation/mean
[b]S-W Statistic: Shapiro-Wilk statistic
[c]Prob Normal: probability the data are from a normal distribution by Shapiro-Wilk test

Twenty-three residences had pre-cleanup average dust lead loadings greater than the HUD benchmark of 40 μg/ft^2. Average post-cleanup dust lead loading in residences with average pre-cleanup loadings above the HUD benchmark of 40 μg/ft^2 were approximately 120 μg/ft^2 lower than average pre-cleanup loadings. The cleanup program reduced the average dust lead leading in 21 out of the 23 residences, a success rate of approximately 91%.

B.2.2.2 Effect of floor level / pre-cleanup average dust lead loading on the reduction in dust lead levels

The reduction in lead loadings (on a percent change basis) was related to building floor number, through an effect of floor number on pre-cleanup mean dust lead loadings. Lower floors tended to have higher pre-cleanup lead loadings[5] and, therefore, showed greater reduction in loading (discussed further in Section B.4.3). Of the 36 residences with pre-cleanup means greater than the HUD screening level of 25 μg/ft^2, 17 of them were located on lower floors (i.e., ≤ 3rd floor), 14 on floors between the 4th and 10th floors, and 5 at floors greater than the 10th (two at 11 and one at 12). Figure B-5 shows a plot of the log-transformed pre-cleanup means vs. floor number; higher average pre-cleanup loadings tended to occur in residences that are located on floors 10 and lower.

In the following analysis, floor numbers are used as a surrogate for pre-cleanup average concentration. Typically, 30 observations or more are desired for making statistical comparisons between two or more groups of data. None of the floor levels had 30 observations and just six floor levels had 10 or more observations (i.e., differences between pre- and post-cleanup dust lead loadings). Therefore, floor levels were combined into three groups: the first group (*lower*) consisting of basement through 3rd floor residences, second group (*middle*) consisting of floors 4 through 10, and the third group consisting of all residences in floors 11 and up (*upper*). Statistics for the pre-cleanup average dust lead loadings for each floor group are shown in Table B-5; Table A-4 provides additional statistics for this data. The data show moderate to high variability, and large positive skewness; log-transformation substantially improved normality for all three floor

---

[5] Older buildings in lower Manhattan tend to have fewer floors than newer buildings. The tendency for lower floors to contain higher pre-cleanup lead loadings may be attributable, at least in part, to the age of the building.

groups. The differences between the means of the pre-cleanup average dust lead loading between the lower and upper floor groups (25.3 $\mu g/ft^2$) is statistically significant

Table B-3. Statistics for Average Pre-cleanup Residential Dust Lead Loading by Floor Group (µg/ft^2).

The tendency for average dust lead loadings to decrease with increasing floor level is indicated by the statistics shown in the table. Also shown is a tendency for the variance to increase with increasing average dust lead loading. When grouped by floor level, the average pre-cleanup dust lead loadings show less variation and are less skewed than the complete distribution of average residential dust lead loadings. A log-transformation of the averages substantially improves the fit of a normal distribution to the data (S-W statistic for lower floor group=0.95, p=0.0149; middle: S-W statistic=0.96, p=0.0127; upper: S-W statistic=0.90 , p<0.0002). Outliers were removed from the dataset (see Section 3.4.1 for details).

Statistic	Floor Group[a]		
	Lower	Middle	Upper
n	61	93	60
Minimum	1.86	1.86	1.86
Maximum	748.95	413.87	294.33
Median	9.20	10.03	7.25
Mean	39.52	21.08	14.18
Standard deviation	102.71	46.41	37.98
Skewness	5.84	6.97	7.06
CV[b]	2.60	2.20	2.68
S-W Statistic[c]	0.36	0.34	0.25
Prob Normal[d]	<0.0001	<0.0001	<0.0001

[a]Floor Group: Lower=floors ≤3; Middle=3 < floors ≤10; upper=floors >10
[b]CV=coefficient of variation=standard deviation/mean
[c]S-W Statistic: Shapiro-Wilk statistic
[d]Prob Normal: probability the data are from a normal distribution by Shapiro-Wilk test

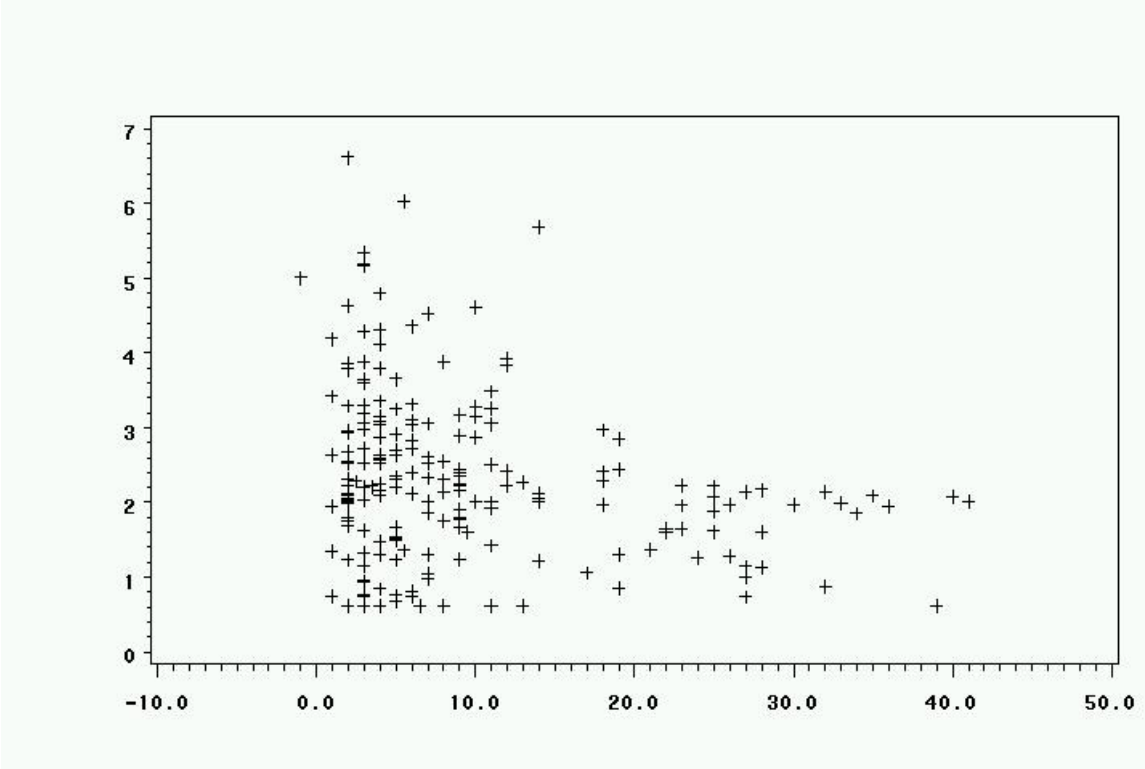

Figure B-5. Scatter plot of log-transformed pre-cleanup residential average dust lead loadings (vertical axis), by floor. The plot indicates that the pre-cleanup average residential dust lead loading decreases with increasing floor levels up to approximately floor level of 15. The mean and variability in pre-cleanup average dust lead loading is fairly constant at floors higher than 15.

(t-test with log-transformed data = 2.60, p=0.0104); the difference between the medians of the lower and upper floor groups is statistically significant by the Mann-Whitney test (W=1,375, p=0.0185). The difference between the means of the middle and upper floor groups (6.9 μg/ft^2) is statistically significant (t-test with log-transformed data = 2.22, p=0.0281); the difference between the medians of the middle and upper floor groups is statistically significant by the Mann-Whitney test (W=2,067, p=0.0069).

As expected, the reduction in dust lead loading in μg/ft^2, and on a percent decrease basis, varied by floor level (i.e., pre-cleanup average loading) (Tables B-4 and B-5). The differences in the reductions in dust lead loading between the lower and upper floor groups, and the middle and upper floor groups were found to be significant by the nonparametric Mann-Whitney test (W=986.0, p=<0.0001; W=2034.5, p=<0.0048, respectively). Prior to estimating the difference in the percent reduction in dust lead loadings between the different floor groups, two observations with extreme negative percent reductions were removed from the data set (see Section B.4.1 for details). The differences in the percent reductions in dust lead loading between the lower and upper floor groups, and the middle and upper floor groups of were found to be significant by the Mann-Whitney test (W=934.5, p=<0.0001; W=1978.5, p=<0.0051, respectively). The cleanup program was successful in reducing the dust lead loading in residences with the highest pre-cleanup average loadings (i.e., located on floor numbers 3 and lower) by approximately 33.1 μg/ft^2, or 43.5 % (95% CI,[3] 17.8, 78.9 μg/ft^2; 29.71, 53.39%). Average residential dust lead loadings in the middle floors were reduced on average by 11.1 μg/ft^2, or 23.1 % (95% CI,[3] 4.40, 27.14 μg/ft^2, 17.42, 39.55 %, respectively). The dust lead loading in floors higher than 10 were reduced on average by 6.9 μg/ft^2, or 8.6% (95% CI,[3] 1.44, 28.54 μg/ft^2, -2.70, 18.35 %, respectively).

B.2.3 Reductions in dust dioxin loadings

The measurable effect of the cleanup program on dust dioxin loadings was less than it was for lead due primarily to low pre-cleanup dust dioxin loadings, which limits the usefulness of the dioxin data to assess the efficacy of the dust cleanup program For this reason, the analysis of the dioxin results is less extensive than the analysis of the lead results.

Pre-cleanup and post-cleanup dust wipe samples for dioxin were collected from 212 apartments, located in 145 buildings. Table B-6 provides statistics for the pre-cleanup and post-cleanup dioxin wipe data; a more complete set of statistics is provided in Appendix A, Table A-5 and A-5a. On average, three pre-cleanup and three post-cleanup wipe samples were collected from each apartment (see Section 2.2 for

Table B-4. Reduction in Dust Lead Loading by Floor Group (µg/ft^2).

The mean reduction in average residential dust lead loading varies by floor level, as expected given the large variation in average pre-cleanup dust lead loadings between the floor groups. The difference in the reduction between the lower and upper floor groups, and between the middle and upper floor groups, are statistically significant (see Section 3.3.2.3 for details). A log-transformation of the averages fails to improve the fit of a normal distribution to the data (S-W statistic for lower floor group=0.41, $p<0.0001$; middle: S-W statistic=0.41 , $p<0.0001$; upper: S-W statistic= 0.27 , $p<0.0001$). Outliers were removed from the dataset (see Section 3.4.1 for details).

Statistic	Floor Group[a]		
	Lower	Middle	Upper
N	61	93	60
Minimum	-6.18	-163.27	-22.18
Maximum	708.21	408.96	289.03
Median	3.94	2.37	0.51
Mean	33.11	11.10	6.94
Standard deviation	97.77	48.91	38.14
Skewness	5.85	5.61	7.10
CV	2.95	4.40	5.50
S-W Statistic	0.35	0.37	0.25
Prob Normal	<0.0001	<0.0001	<0.0001

[a]Floor Group: Lower=floors ≤3; Middle=3 <floors ≤10; upper=floors >10
[b]CV=coefficient of variation=standard deviation/mean
[c]S-W Statistic: Shapiro-Wilk statistic
[d]Prob Normal: probability the data are from a normal distribution by Shapiro-Wilk test

Table B-5. Percent Reduction in Average Residential Dust Lead Loading by Floor Group (µg/ft^2).

The percent reduction in average residential dust lead loading varies by floor level. The difference in the reduction between the lower and upper floor groups, and between the middle and upper floor groups, are statistically significant (see Section 3.3.2.3 for details). The negative skewness for each floor level is due to a few increases in average dust lead loading after cleanup. In addition to the two observations that were removed as outliers (see Section 3.4.1), two residences were removed from the this analysis as outliers; the average post-cleanup dust lead loading in these residences were 484% and 448% higher than the pre-cleanup average (i.e., increased from 4.4 to 25.9, and 4.9 to 27.1 µg/ft^2, respectively).

Statistic	Floor Group[a]		
	Lower	Middle	Upper
N	61	92	59
Minimum	-180.10	-208.25	-149.79
Maximum	95.41	98.82	98.20
Median	57.39	29.24	6.94
Mean	43.48	23.13	8.64
Standard deviation	47.02	54.51	41.71
Skewness	-1.84	-1.69	-0.70
CV	1.08	2.36	4.83
S-W Statistic	0.83	0.87	0.95
Prob Normal	<0.0001	<0.0001	<0.0085

[a]Floor Group: Lower=floors ≤3; Middle=3 < floors ≤10; upper=floors >10
[b]CV=coefficient of variation=standard deviation/mean
[c]S-W Statistic: Shapiro-Wilk statistic
[d]Prob Normal: probability the data are from a normal distribution by Shapiro-Wilk test

Table B-6. Statistics for Dioxin Wipe *Clean and Test* Data (ng/m^2).

The data summarized in the above table are dioxin toxicity equivalents (TEQs), which are the sum of 17 different chemical forms (congeners) of dioxin. The *clean and test* subset of the data exhibit high positive skewness but low variance. Few exceedances were observed for dioxin. The raw data and log-transformed pre- and post-cleanup data fail the S-W test for normality (log-transformed data [pre-/post-]: S-W statistic=0.71/0.89, p<0.0001/p<0.0001).

Statistic	Pre-cleanup	Pre-cleanup[a]	Post-cleanup
Apartments sampled	213	213	213
Buildings sampled	145	145	145
Number of samples	674	673	668
Nondetects	162 (24.0%)	162 (24.1%)	228 (34.1%)
Exceedances[b]	3 (0.4%)	2 (0.3%)	4 (0.6%)
Minimum	0.27	0.27	0.27
Median	0.60	0.60	0.59
Mean	0.81	0.66	0.65
Maximum	103	5.14	4.34
Standard deviation	3.95	0.29	0.28
Skewness	25.75	6.79	5.27
CV[c]	0.49	0.44	0.42
S-W Statistic[d]	0.03	0.57	0.62
Prob Normal[e]	<0.0001	<0.0001	<0.0001

[a]Statistics for pre-cleanup data with one outlier removed (see Section B.2.3 for details).
[a]Exceedance: dioxin wipe samples that exceeded the health-based benchmark of 2 ng/m^2 TEQ EMPC (ND=1/2).
[b]CV=coefficient of variation=standard deviation/mean
[c]SW-Statistic: Shapiro-Wilk statistic
[d]Prob Normal: probability the data are from a normal distribution deviation/mean

a description of the cleanup program). The dioxin loading measured in one sample collected from a fireplace mantle had a value of 75.3 ng/m^2, approximately 20 times higher than the next highest value (5.14 ng/m^2). This sample was removed from the data set as an outlier. The pre- and post-cleanup data exhibit moderate variance and positive skewness, and the normal distribution is found to be a poor fit to the data (Figure B-6). A log-normal transformation of the data fails to substantially improve normality. Given the low levels of dioxin that were found prior to cleanup, the mean and median of the post-cleanup data are very similar to the mean and median of the pre-cleanup data.

Table B-7 presents statistics on the average pre-cleanup, average post-cleanup and average reduction in dust dioxin loadings, on a residence-by-residence basis. The distribution of the reductions is moderately negatively skewed with high variance (Figure B-7). Tests for normality indicate the normal distribution provides a poor fit to the data. A log-normal transformation of the data fails to improve normality (S-W=0.85, $p<0.0001$).

On average, the cleanup program reduced the average dioxin loading by approximately 0.01 ng/m^2 (95% CI,[3] –0.0161, 0.0327%). The inclusion of zero within the CI indicates that the reduction in dust dioxin loading is not significant. However, the sign test (M=14, p=0.06) and, particularly, the Wilcoxon signed rank test (S=1,790, p=0.05), indicate that the reduction in dust dioxin loadings was significant. The Wilcoxon signed rank test will tend to be more powerful at detecting differences between the pre-cleanup and post-cleanup average dust dioxin loadings than the sign test provided that the distribution of the differences in dust dioxin loading is symmetric (but not necessarily conforming to a normal distribution) (Conover, 1999). Based on Figure B-7, the assumption of symmetry appears to be reasonable.

The post-cleanup average dioxin loading was greater than the pre-cleanup average in 92 residences, and lower in the other 120 residences, yielding a rate of reduction of approximately 57 %. The sign test (see preceding paragraph) indicates that the rate at which the cleanup program lowered the average residential dust dioxin loading is statistically significant.

To assess the effectiveness of the dust cleanup program for residences that had measurable pre-cleanup dust dioxin loading, the comparison between residential average pre-cleanup dust dioxin loadings and residential average post-cleanup dust dioxin loadings was limited to residences where all the pre-cleanup measurements for dioxin were above the detection limit. There were

124 residences In 93 buildings that met this criterion. The pre-cleanup measurement of 75.3 ng/m^2 was not included in this data set (see preceding section). The cleanup program reduced the residential average dust dioxin loading in these

Table B-7. Reduction in Average Dioxin Wipe Loadings (TEQ)[a] (Pre- and Post-cleanup) (ng/m^2).

The reductions in average residential dust dioxin loadings are more modest than the reductions achieved for average dust lead loading, primarily due to the low average pre-cleanup dust dioxin loadings. Analysis of the reduction in the residential average dust dioxin loading in a subset of the 212 residences, where all pre-cleanup sample measurements results were greater than the detection limit, also indicated an average reduction of 0.01 ng/m^2.

Statistic	Reduction in Average Dioxin Wipe Loading	Average Pre-cleanup Dioxin Wipe Loading	Average Post-cleanup Dioxin Wipe Loading
n	212	212	212
Mean	0.01	0.65	0.64
Standard deviation	0.18	0.18	0.19
Skewness	-0.97	1.88	2.06
CV[b]	19.02	0.28	0.30
Var	0.03	0.03	0.04
Maximum	0.63	1.61	1.36
Median	0.01	0.60	0.60
Minimum	-0.81	0.33	0.32
S-W Statistic[c]	0.85	0.83	0.78
Prob Normal[d]	<0.0001	<0.0001	<0.0001

[a]TEQ: toxicity equivalent quotient.
[b]CV=coefficient of variation=standard deviation/mean
[c]S-W Statistic: Shapiro-Wilk statistic
[d]Prob Normal: probability the data are from a normal distribution by Shapiro-Wilk test

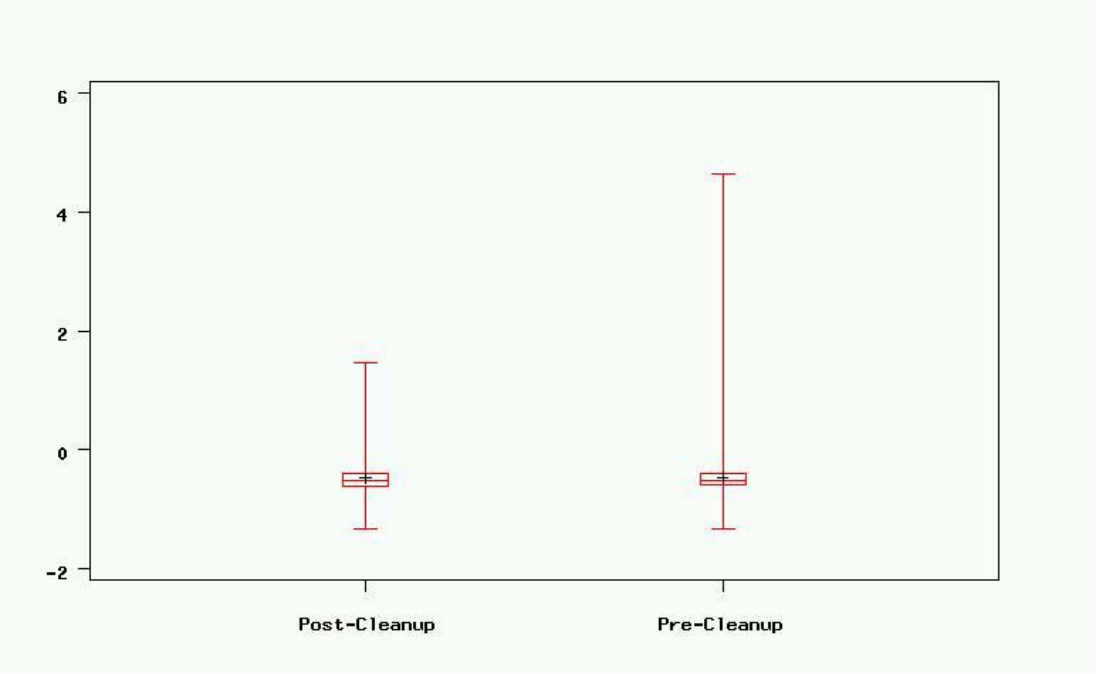

Figure B-6. Boxplots for residential dust dioxin loading (μg/ft^2), by sample type. The distributions of the pre- and post-cleanup average dust dioxin loadings also exhibit extreme positive skewness. No pre- or post-cleanup average dust dioxin loadings exceeded the health-based benchmark of 2 ng/m^2. One observation, with a value of 103 ng/m^r, was removed from the data as an outlier. This observation was collected from the mantle of a fireplace.

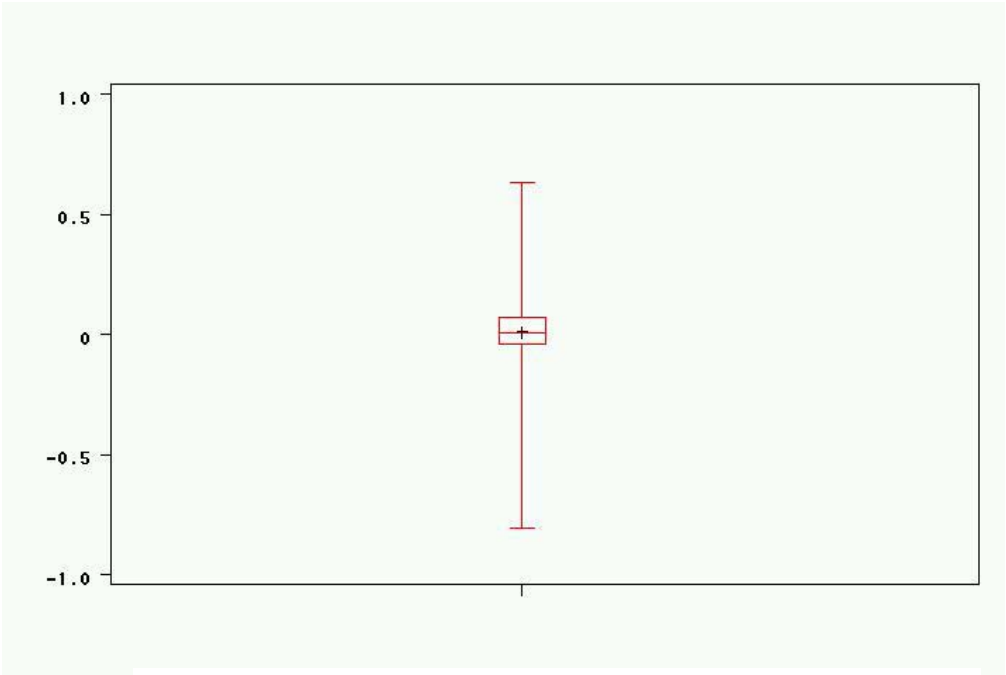

Figure B-7. Boxplot for the reduction in residential average dioxin wipe reductions. The short length of the 'box' indicates the most of the reductions are close to zero. The small reductions are due to the low pre-cleanup average dust dioxin loadings in all but one of the residences (the residence with the one high pre-cleanup dioxin dust loading of 103 ng/m^2). One observation, with a value of 103 ng/m^r, was removed from the data as an outlier. This observation was collected from the mantle of a fireplace.

124 residences by approximately 0.01 ng/m^2, the same average reduction that was observed in the 212 residences.

B.3 SPATIAL PATTERN OF PCME EXCEEDANCES

B.3.1 Analytical approach

B.3.1.1 Purpose

Data were analyzed to detect the possible presence of spatial, or geographic patterns in the occurrence of PCMe exceedances. In this report, a PCMe exceedance is defined as a sample result that exceeded the heath-based benchmark of 0.0009 fibers/cc. Detection of spatial patterns in the exceedances could be used to identify possible sources of the exceedances, or lead to explanations for the exceedances. The latter could be used to improve future cleanup and/or monitoring efforts. The data were divided into two groups: data from residences and building common areas that were cleaned and tested (*clean and test* data), and data from residences that were tested only (*test only* data). All common areas (e.g., lobbies, laundry rooms, hallways, stairwells) were cleaned and tested.

B.3.1.2 Analytical Methods and Spatial Resolution

The methods that are used to detect and measure spatial patterns depend upon the spatial scale and resolution at which the spatial patterns are analyzed. The spatial scale refers to the geographic extent over which the analysis is performed. In this report, the geographic scale is lower Manhattan, south of Canal Street (Figure 1-1). Regarding geographical scale, the pattern of PCMe exceedance could be analyzed by examining the buildings where the health-based benchmark was exceeded, or by examining the number, or rate of exceedances over larger geographic areas. As resolution decreases, the data must be aggregated (e.g., summed, averaged) over the chosen geographic units (e.g., zip codes), which results in some loss of geographic information (i.e., the exact location where the individual exceedances occurred). However, aggregating the data tends to reduce variability, which may then reveal spatial patterns that had been obscured by small-scale variability in the data (i.e., fluctuations in the data over short distances).

The appropriate spatial scale and resolution depends upon the objectives of the analysis. For example, one of the objectives of this analysis was to determine if the geographic location of PCMe exceedances were clustered geographically. For this objective, the PCMe data were analyzed at the site level and the building level (the latter being the smallest geographic unit reported). The second objective was to determine if the rate of PCMe exceedance (i.e., number of exceedances/number of samples analyzed) varied across the area that was potentially affected by the collapse of the WTC buildings. For this objective, the PCMe data were aggregated over statistical summary areas (SSAs) (Figure 1-1). Statistical summary areas were based on census-block groups that were modified by EPA for the purposes of describing the PCMe data.

Spatial pattern analyses at the site level and building level were performed using methods of point pattern analysis (Cressie, 1993; Bailey and Gatrell, 1995). In point pattern analysis, the focus is on the location of exceedances. The goal is to determine if there are any geographic patterns exhibited by the location of the exceedances. In general, there are two types of geographic patterns that are possible: clustering and dispersion (or regularity). Clustering is exhibited by the tendency for points to be located in clumps, while dispersion refers to the tendency for points to be more regularly distributed than would be expected, based on chance. An example of a point pattern that exhibits dispersion is a square grid. The primary focus in this study is on identifying clusters of exceedances, which could indicate an asbestos source, or otherwise lead to an explanation for the elevated air borne asbestos concentrations.

Analysis of the PCMe data at the SSA scale was performed using methods from spatial autoregression analysis. Spatial autoregression is a type of statistical regression analysis that considers the spatial autocorrelation exhibited by the data, if any. In the present context, (positive) spatial autocorrelation is the tendency for SSAs with similar rates of PCMe exceedances to be located near each other. Classical regression analysis assumes the data are independent and identically distributed (iid)[6]. Data that exhibit spatial autocorrelation violate the

[6] Many methods of classical statistical analysis are developed mathematically based, in part, on the assumption that the data are independent and identically distributed. The assumption of independence requires that the probability that an observation from the sample takes on a given value is not dependent upon the values of any of the other observations. The identically

independent portion of this assumption. Therefore, using classical regression methods with data that exhibits spatial autocorrelation will affect the accuracy of statistical tests that are made with the data; for example, testing the rates of PCMe exceedances between SSAs could lead to erroneous conclusions.

B.3.1.3 PCMe Exceedance as a Spatial Poisson Process

The spatial analysis of the PCMe exceedances that is presented in Sections B.2.2.2 and B.2.3 is based on the assumption that the exceedances can be modeled as a Poisson distribution (Figures B-8 and B-9). The rationale for this assumption is as follows.

The spatial analysis of the PCMe data focuses on the spatial distribution of PCMe exceedances, rather than on the spatial distribution of the PCMe concentration. When analyzed in this way, the PCMe data are converted into one of two values: one (concentrations > 0.0009 f/cc) or zero (concentrations < 0.0009 f/cc). In this format, the data can be modeled with a binomial distribution (DeGroot, 1989):

$$f(x \mid n, p) = \binom{x}{n} p^{x} (1-p)^{n-x} \qquad \text{Equation B-1}$$

The expression on the left hand side of Equation B-1 is interpreted as the probability of observing x exceedances out of n air samples (i.e., tests), given the probability of observing an exceedance from any given test (p). The variable x therefore is limited to positive integers between zero and the sample size (i.e., $x = 0, 1, 2, \ldots, n$). The parameter p is estimated from the data; it is the total number of exceedances divided by the number of samples (n). The $\binom{x}{n}$ symbol represents the number of *combinations* of n objects taken x at a time[7]. Assuming a binomial distribution

---

distributed assumption requires that all of the observations are members of the same population (i.e., the same distribution function).

[7] In the present context, it represents the number of ways that x exceedances could be observed in n samples, when order is not important. The right hand side of equation 1A equals the number of ways that x exceedances could be observed in a sample of size n, multiplied by the probability of observing an exceedance for any given test.

provides a good fit to the PCMe exceedance data, the expected number of exceedances, given n samples and probability p is:

$$E[X] = np \qquad \text{Equation B-2}$$

and its variance of x is:

$$Var[X] = np(1 - p) \qquad \text{Equation B-3}$$

Notice that the number of exceedances will tend to increase with sample size. The variance also increases with sample size. The relationship between variance and sample size must be considered when

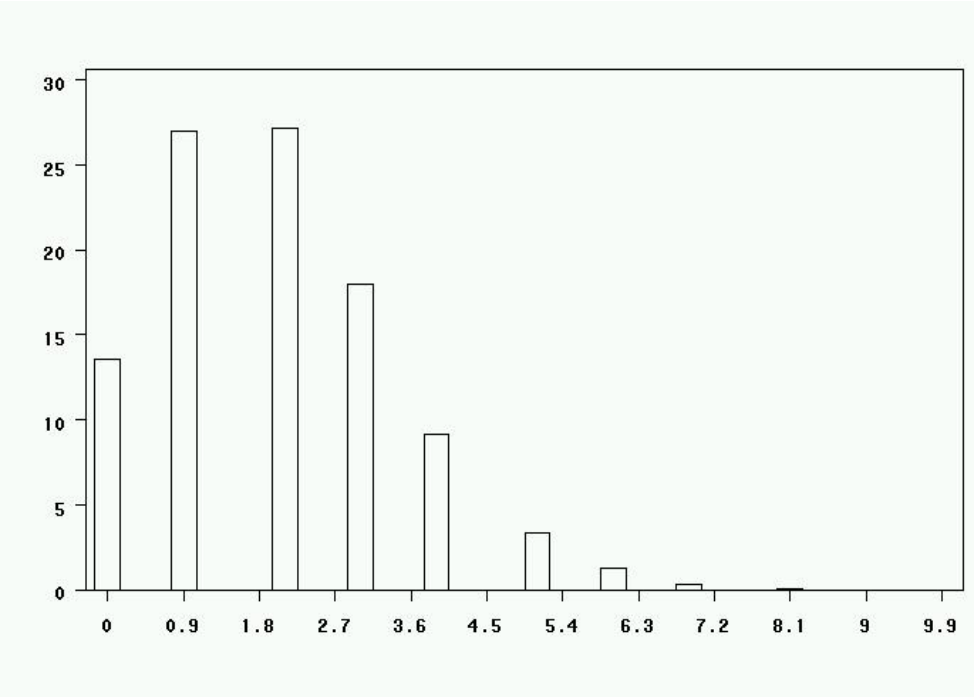

Figure B-8. Histogram for 10,000 randomly generated samples from a Poisson distribution with mean = 2. The value of the sample is shown on the x-axis, the y-axis shows the percent of the 10,000 samples that have the value indicated on the x-axis. A Poisson distribution is commonly used to model the occurrence of rare events within a fixed period of time or space. The Poisson distribution with mean = 2 is positively skewed; as the mean of a Poisson random variable increases, its distribution approaches a normal distribution.

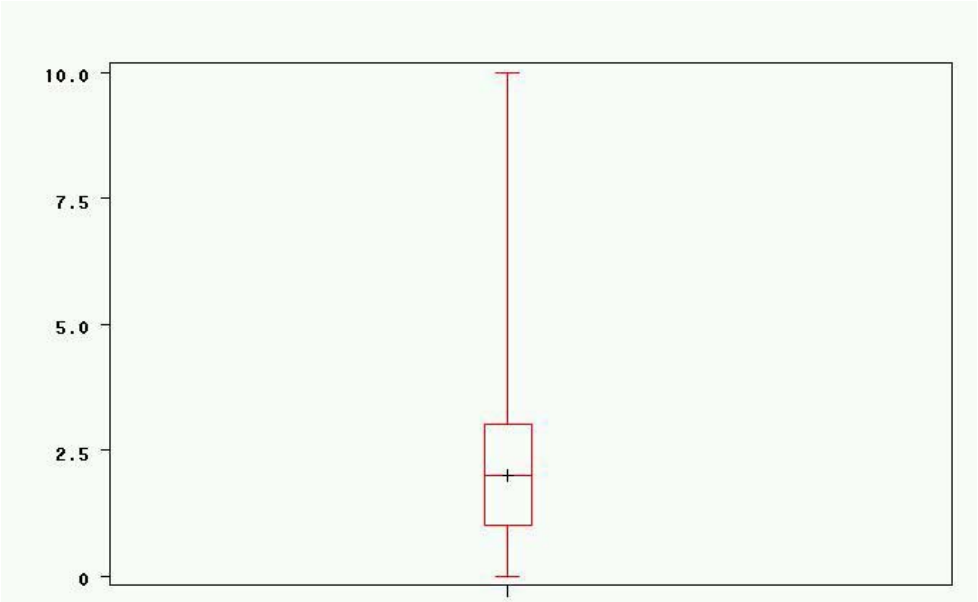

Figure B-9. Boxplot for 10,000 randomly generated samples from a Poisson distribution with mean = 2. The values of the randomly drawn samples are shown on the y-axis. As shown above, the boxplot for a Poisson distribution is positively skewed. As the mean of a Poisson random variable increases, its distribution approaches a normal distribution.

comparing exceedance rates between areas with different sample sizes; this point is discussed further in Section B.3.2.2.

The binomial distribution can be approximated with a normal distribution. The advantages of modeling the exceedances with a normal distribution is that there are many statistical procedures that are based on the assumption of normality, and the variance of a normally distributed variable does not depend upon sample size (i.e., the variance is constant). The normal approximation improves as n increases and the value of p approaches 0.5 (DeGroot, 1989). However, the estimates for p for the *test only* and *clean and test* data (0.00487 and 0.00418, respectively), make the normal approximation untenable. For example, the normal approximation would generally be considered acceptable for a comparison of the exceedance rates between SSAs provided the following relationship was satisfied for each of the SSAs:

$$n_{SSA} \times exceedance\,rate_{SSA} > 5$$

where, n_{SSA} is the number of samples in the SSA, and exceedance $rate_{SSA}$ is the number of exceedances located in the SSA divided by n_{SSA}. This requirement would be satisfied for just one SSA for the *test only* data, and five SSAs for the *clean and test* data.

The Poisson distribution was developed for modeling rare events, such as the exceedance rates observed in the WTC cleanup program. When n is large and p is very small, the binomial distribution can be approximated by a Poisson distribution (DeGroot, 1989):

$$f(x \mid \lambda) = \frac{e^{-\lambda}\lambda^{x}}{x!} \qquad \text{Equation B-4}$$

The variable x is limited to positive integers between zero and the sample size (i.e., x = 0, 1, 2, …., n). The parameter λ is estimated from the data; it is the total number of exceedances divided by the number of samples (*n)* (same as the binomial distribution). The mean and variance of a Poisson distribution are equal to the parameter λ, and do not depend upon the sample size. In Section B.3.2.2 the Poisson distribution is shown to provide a better fit to the data than the binomial.

Possible differences in the intensity of exceedance events across the site is assessed in Section B.3.2, using methods from point pattern analysis (Section B.3.2.1) and spatial autoregression (B.3.2.2); possible differences on a smaller scale (e.g., within SSAs) are assessed using additional methods from point pattern analysis (Section B.3.2.3). The effect of sample size (i.e., number of samples per building) on PCMe exceedance is also considered in Section B.3.2.

B.3.2 Spatial Analysis

The locations of PCMe exceedance were described by first assessing the overall (*global*) pattern of the exceedances using methods from point pattern analysis. The data were then aggregated by SSAs and analyzed using methods from spatial autoregression to describe the spatial distribution of PCMe exceedances at the SSA-scale, and to estimate the differences in the rate of PCMe exceedances between the SSAs. The local pattern of the exceedances was assessed by measuring the level of spatial autocorrelation, or spatial dependence, exhibited by the data, using additional methods from point pattern analysis. Finally, the vertical distribution of PCMe exceedances is analyzed at the site level using frequency tables and Poisson regression. When interpreting the results of this analysis, it should be kept in mind that participation in the WTC Dust Cleanup Program was on a voluntary basis. Therefore, the data were not derived from a random sample, nor do they represent a census of all the buildings and residences within the sampled area. (In the context of point pattern analysis, point patterns derived from a random sample and census are referred to as *sampled point patterns* and *mapped point patterns*, respectively.) With this in mind, the global and local patterns of PCMe exceedance are interpreted in relation to the location of the sampled buildings.

B.3.2.1 Site-Level (Global) Pattern of PCMe Exceedance

For the point pattern analysis, the PCMe data were aggregated at the building level by counting the number of sample results that exceeded the heath-based benchmark of 0.0009 fibers/cc for each building (i.e., the number of exceedances). The term *exceedance event* is used to refer to buildings that contain at least one PCMe exceedance. Consistent with the approach used in the analysis of the dust wipe data, the PCMe exceedances were grouped into *clean and test* and *test only* categories. Figures B-10 and B-11 show the location (centroids) of the 408 buildings that

contain at least one residence or common area that was cleaned and tested (*clean and test* buildings*)*, and the 219 buildings that contain at least one residence that was tested only (*test only* buildings), respectively. Note that the two groups of buildings are not mutually exclusive: approximately 39% of the *clean and test* buildings contain at least

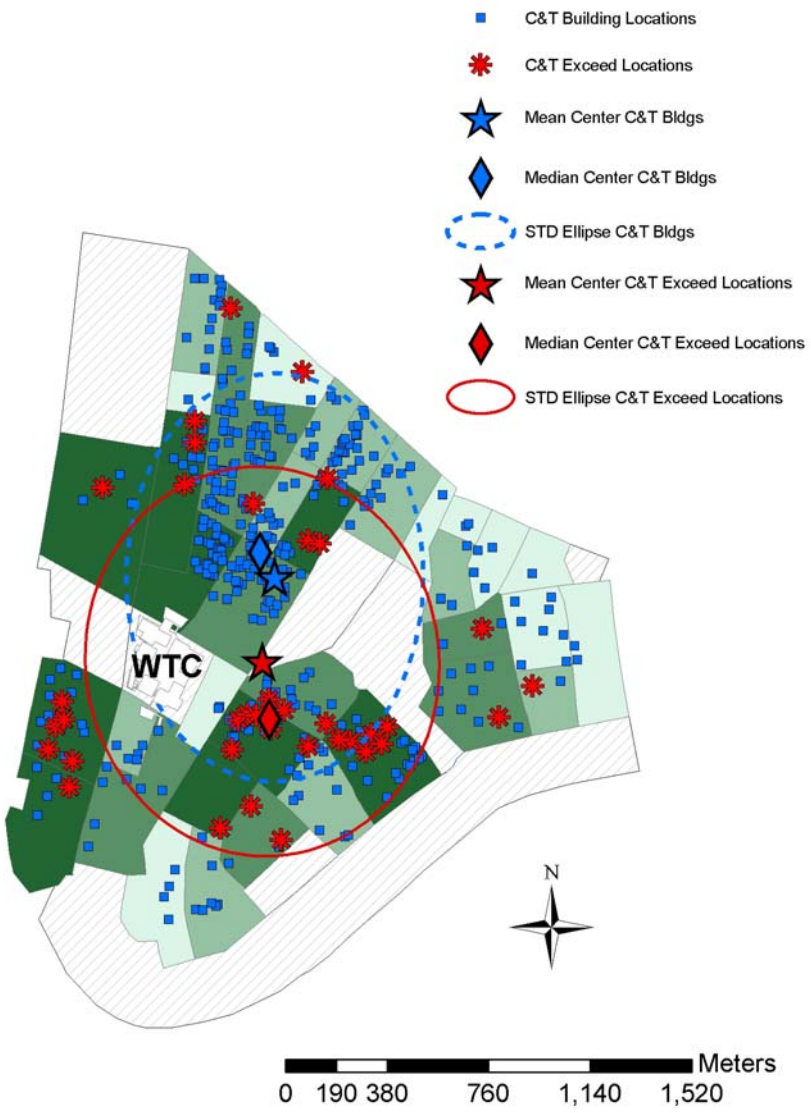

Figure B-10. Centrographic statistics for the *clean and test* data. *Clean and test* data refers to samples collected from re
the residents had requested EPA to clean their residences and test their indoor air for asbestos. Centrographic statistics
dimensional counterparts of common one-dimensional summary statistics; they describe global characteristics of the da
represent statistical summary areas (SSAs); hatching indicates SSAs where PCMe data was not collected. Two-dimensi
statistics are indicated by stars (mean center, or average of X and Y coordinates) and diamonds (median center, median
coordinates). The figure indicates the geographic center of the location of the 37 exceedances is shifted towards the sou
the geographic center of the *clean and test* buildings. Comparison of the median center and the arithmetic mean center
exceedances indicates that the location of the exceedances is 'skewed' slightly towards the north. Comparison of the sta
deviational ellipses, which illustrate the dispersion of events around their mean centers, indicates that the pattern of exc
more evenly distributed across lower Manhattan than the pattern of *clean and test* building locations. The ellipse for the
buildings is more elongated in the north-south direction, indicating that the building locations are more dispersed in the
direction than they are in the east-west direction. The median number of samples collected from *clean and test* building
least one exceedance (119) is an order of magnitude higher than the median number of samples collected from clean and
that had no exceedances (12). The shades of green assigned to the statistical summary areas (SSAs) indicate the numbe
collected from each SSA. The four shades of green correspond to quartiles of the number of samples; the darkest green
SSAs with the largest number of samples (i.e., 4th quartile). There is a strong relationship between the sample size and t
exceedances; 36 of the 38 exceedances are located in SSAs with sample sizes above the median.

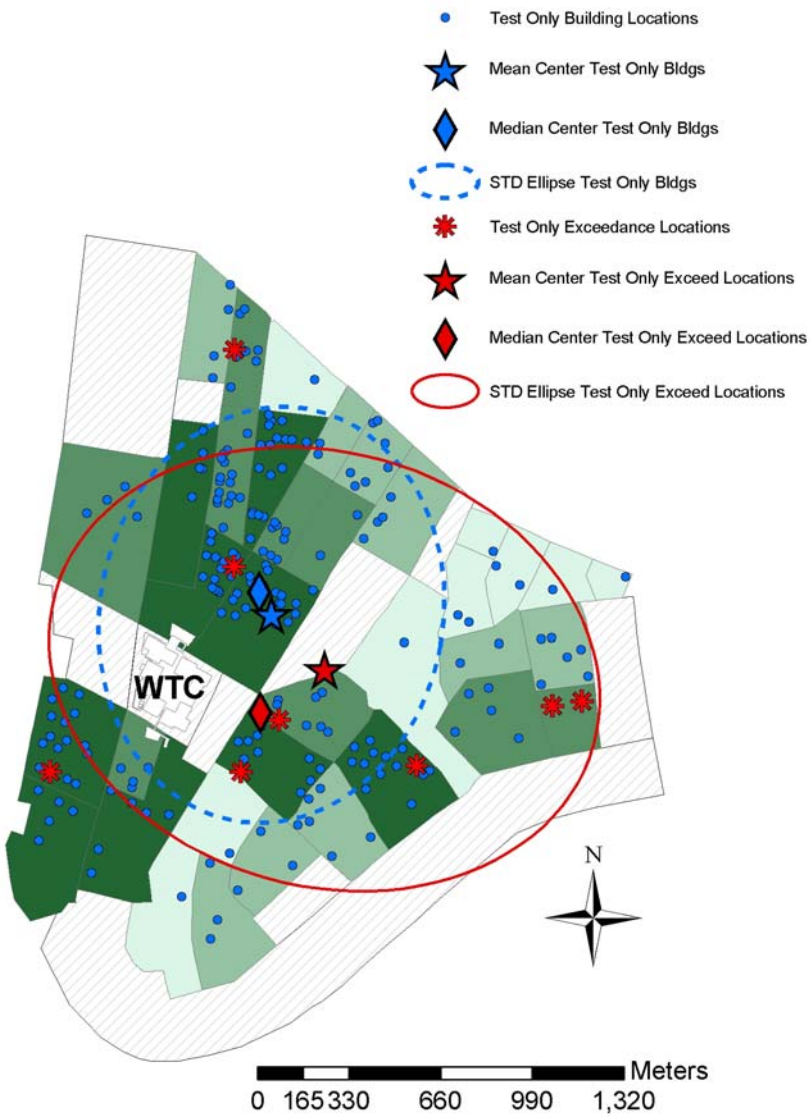

Figure B-11. Centrographic statistics for the *test only* data. *Test only* data refers to samples collected at residents where resid requested to have their indoor air tested for asbestos but declined to have their residences cleaned. The figure indicates th geographic center of the location of the 8 exceedances is shifted towards the south relative to the geographic center of the *test only* buildings. Comparison of the median center and the arithmetic mean center for the exceedances indicates that the location of the exceedances are 'skewed' slightly towards the east. The standard deviational ellipse for the *test only* buildings shows that the exceed are more dispersed in the north-south direction, while the exceedances are dispersed more in the east-west direction. The east-west t may be attributable to the higher sample sizes associated with buildings where the exceedances were measured. The median number samples in the 8 *test only* buildings that had at least one exceedance is 19.5 (range of 9 to 38 samples); the median number of sample the *test only* buildings without exceedances is 7 (range of 3 to 256 samples). The shades of green assigned to the statistical summary (SSAs) indicate the number of samples collected from each SSA. The four shades of green correspond to quartiles of the number of samples; the darkest green is assigned to SSAs with the largest number of samples (i.e., 4th quartile). There is a strong relationship b the sample size and the location of exceedances; all of the exceedances are located in SSAs with sample sizes above the median.

one residence that was tested only, and approximately 75% of the *test only* buildings contain at least one common area or residence that was cleaned and tested.

Centrographic statistics were used to describe the first order, or global pattern of the distribution of the exceedance events. The centrographic statistics that are described here are similar to the traditional univariate statistics that are used to describe the location (e.g., mean, median) and distribution (e.g., standard deviation, skewness) of a single variable. Centrographic statistics were calculated using the geographic coordinates of the centroids of the buildings. Centrographic statistics were used to describe the geographic center of the exceedance events, their distribution in space, and the orientation of the distribution. The centrographic statistics for the exceedance events were then compared to the centrographic statistics for the buildings that were sampled.

Figures B-10, B-11, and B-12 show the mean centers, median centers, and standard deviational ellipses for the *clean and test* buildings and the *clean and test* exceedance events, *test only* buildings and *test only* exceedance events, and the *unique test only* buildings (described below), respectively. The X and Y coordinates of the mean center equal the mean of the X coordinates and the mean of the Y coordinates, respectively, of the building centroids. The coordinates of the median center equal the median of the X and Y coordinates of the building centroids. The median is less influenced by geographic outliers (buildings that are located far from the median or mean center of buildings) than the mean. The median is often used when there are a few extreme locations that could greatly influence the mean and distort what might be considered the geographic center of the building locations.

A standard deviational ellipse is a measure of the dispersion of the buildings around the mean center in two dimensions. Comparing the standard deviational ellipse for the exceedance events to the standard deviational ellipse for the location of the sampled buildings provides a qualitative comparison between their geographic centers, and the magnitude and direction of their dispersion. The method for calculating the standard deviational ellipse is described in Appendix C.

Figure B-11 shows the locations of the 219 *test only* buildings and 8 exceedance events (one exceedance event is obscured by the symbol for the median center of the exceedance events). The mean center for the exceedance events, which is shifted to the east and north of the median center, is influenced by the two exceedance events that are located near the eastern boundary of the potentially affected area, and the one event near the northern boundary. The location, shape

and approximately north-south orientation of the standard deviational ellipse for the *test only* buildings reflect the high density of

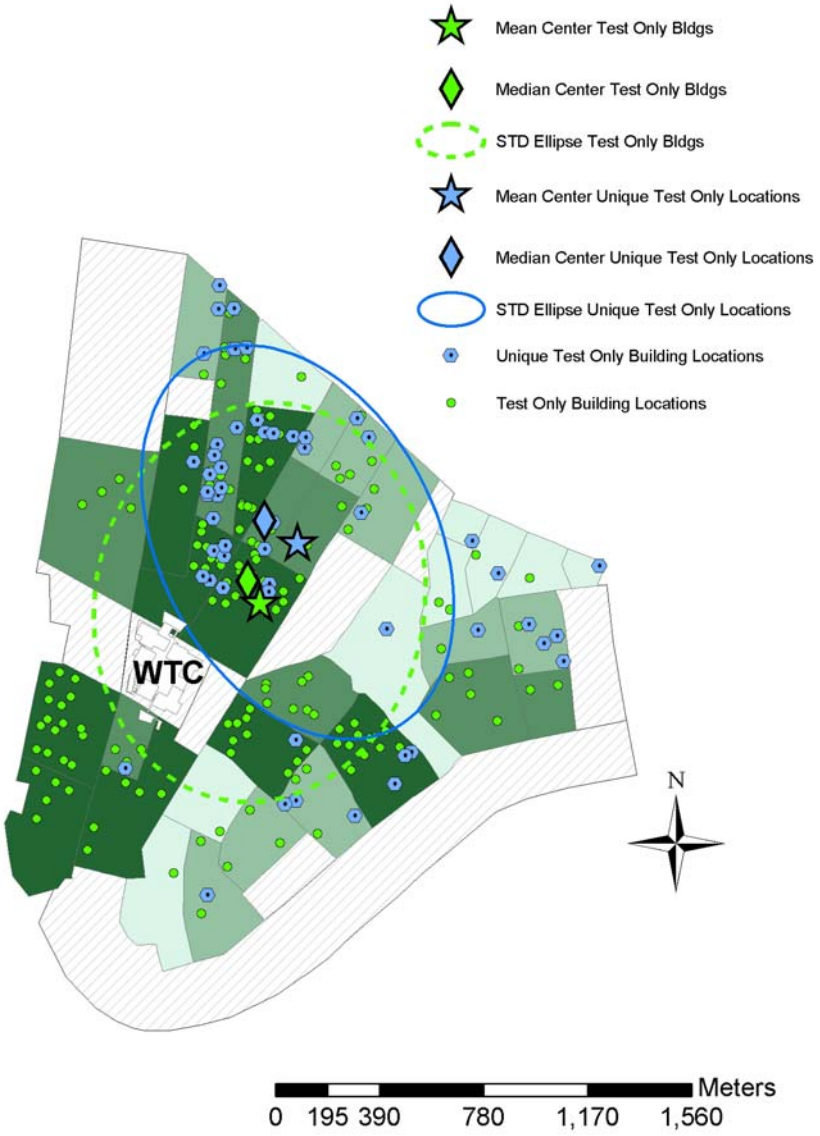

Figure B-12. Centrographic statistics for the *unique test only* buildings. *Unique test only* buildings are buildings that do not contain any residences or common areas that were cleaned. The *unique test only* buildings tend to be located north of the *test only* buildings, and are dispersed in a northeast-southwest direction. No PCMe exceedances were measured in any unique test only building. The lack of exceedance events could be attributed, in part, to the low number of samples collected from these buildings. The average number of samples collected from the *unique test only* buildings is 6.5, with a minimum of 3 and a maximum of 12; twenty-three of the 54 *unique test only* buildings had 5 or fewer samples, and 47 had fewer than 10. In contrast, the 8 *test only* buildings with one or more exceedance had an average of 22 samples, with a minimum of 6 and a maximum of 38. The shades of green assigned to the statistical summary areas (SSAs) indicate the number of samples collected from each SSA. The four shades of green correspond to quartiles of the number of samples; the darkest green is assigned to SSAs with the largest number of samples (i.e., 4th quartile).

sampled buildings that are located northeast, east and southwest areas of the WTC site. In contrast, the spatial pattern of the *test only* exceedances events approaches an east-west oriented line; the lone exceedance event located near the northern boundary of the site has a very large influence on the shape of the ellipse. The east-west trend indicated in Figure B-11 may be attributable to the higher sample sizes associated with buildings where the exceedances occurred. The median number of samples in the 8 *test only* buildings that had at least one exceedance is 19.5 (range of 9 to 38 samples); the median number of samples for the *test only* buildings without exceedances is 7 (range of 3 to 256 samples).

Figure B-12 shows the location of the 60 buildings that contain exclusively *test only* residences (*unique test only*; i.e., no *clean and test* common areas or residences). There were no exceedances in the *unique test only* buildings. The geographic center of the *unique test only* buildings shows that these buildings tend to be located north of the *test only* buildings. It should be noted that the lack of exceedance events could be attributed, in part, to the low number of samples collected from these buildings. The median number of samples collected from the *unique test only* buildings is 6, with a minimum of 3 and a maximum of 21; 24 of the 60 *unique test only* buildings had 5 or fewer samples collected from them, and 52 had fewer than 10.

Figure B-10 shows the locations of the 408 *clean and test* buildings and the 37 exceedance events. The geographic center of the *clean and test* buildings is located northeast of the WTC site. The geographic center of the *clean and test* buildings that had at least one exceedance is located east of the WTC site, and south of the geographic center of the *clean and test* buildings. The standard deviational ellipse for the *clean and test* buildings and the *clean and test* exceedances both indicate a north-south orientation. The width of the standard deviational ellipse for the *clean and test* exceedances is wider than the ellipse for the *clean and test* buildings, indicating the distribution of exceedances are more dispersed in the east-west direction than are the *clean and test* building locations. The intensity of exceedances appears to be greater south and east of the WTC site compared to the areas north of the WTC site. Again, the apparent pattern may be attributable, at least in part, to differences in sample size. The median number of samples collected from *clean and test* buildings that had at least one exceedance (119) is approximately 10 times higher than the median number of samples collected from *clean and test* buildings that had no exceedances (12).

The geographic center of the exceedance events for the *test only* and *clean and test* buildings tend to be located south of the geographic center of the sampled buildings (Figure B-10). Except for one location, the *test only* exceedance locations occur along an east-west line that extends across lower Manhattan (Figure B-11). No obvious pattern to the *clean and test* exceedances is evident. Interpretation of the exceedance locations is complicated by the variability in the number of samples that were collected between buildings.

The possible differences in intensity of exceedance events across the site were further addressed using methods from spatial autoregression (Section B.3.2.3) and using additional methods from point pattern analysis (Section B.2.2.3). The effect of sample size (i.e., number of samples per building) on PCMe exceedance is also considered in both of the analyses.

B.3.2.2 SSA-Level Pattern of PCMe Exceedance

Spatial distribution of PCMe Exceedance

The primary objective of this analysis is to describe the spatial distribution of PCMe exceedances at the SSA-scale, and to estimate the differences in the rate of PCMe exceedances between the SSAs. Samples from *test only* and *clean and test* residences were collected from 36 and 38 SSAs, respectively. Rates were calculated for each SSA as the number of exceedances within the SSA divided by the number of results for PCMe for the SSA. Rates were used to account for the large difference in sample sizes between the SSAs.

Exceedance rates varied from 0 to 0.060 for the *test only* data and from 0 to 0.058 for the *clean and test* data. More than one-half of the SSAs had no exceedances for the *test only* (30/37, or 81% with 0 exceedances) and *clean and test* data (23/39, or 60% with 0 exceedances). The spatial distribution of the PCMe exceedance rates for the *test only* and *clean and test* data are shown in Figures B-13 and B-14, respectively. For the *test only* data, the SSAs with the highest rates (upper quartile) coincide with the distribution of the exceedance events; every SSA with one or more exceedance falls in the upper quartile of the exceedance rate, which further indicates the rareness of the exceedance events. SSAs that fell within the upper quartile contained 1 – 9 exceedance events.

For the *clean and test* data, SSAs that fell within the upper quartile of exceedance rates for the *clean and test* data contained 2 to 32 exceedance events. All but 4 SSAs had exceedance rates less than 1%; the highest rate of exceedances was 6%. Statistical summary areas with the highest rates are located north and east of the WTC site. Figure B-14 indicates there is a tendency for SSAs with similar rates to be located near each other (i.e., positive spatial autocorrelation). Measuring spatial autocorrelation in

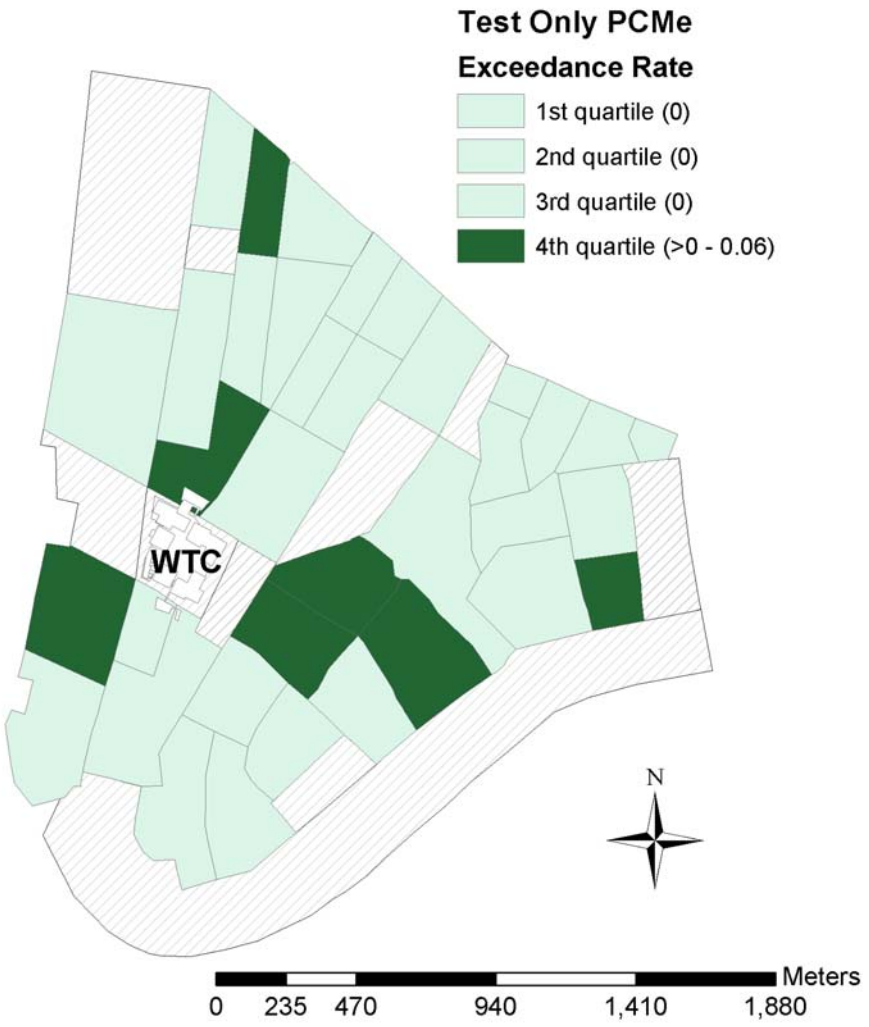

Figure B-13. Spatial distribution of PCMe exceedance rates for the *test only* data, by statistical summary areas. *Test only* data refers to samples collected at residents where residences requested to have their indoor air tested for asbestos but declined to have their residences cleaned. The exceedance rate for each statistical summary area (SSA) equals the number of PCMe results for the SSA that exceeded the health-based benchmark, divided by the number of samples collected from the SSA. Quartiles of the PCMe exceedance rate are shown. Statistical summary areas with one or more PCMe exceedance fall in the upper quartile of the exceedance rate, which indicates the rareness of the exceedance events. Six of the seven SSAs that had one or more exceedance are located east and north of the WTC site; the seventh SSA, which is located south west of the WTC had one exceedance.

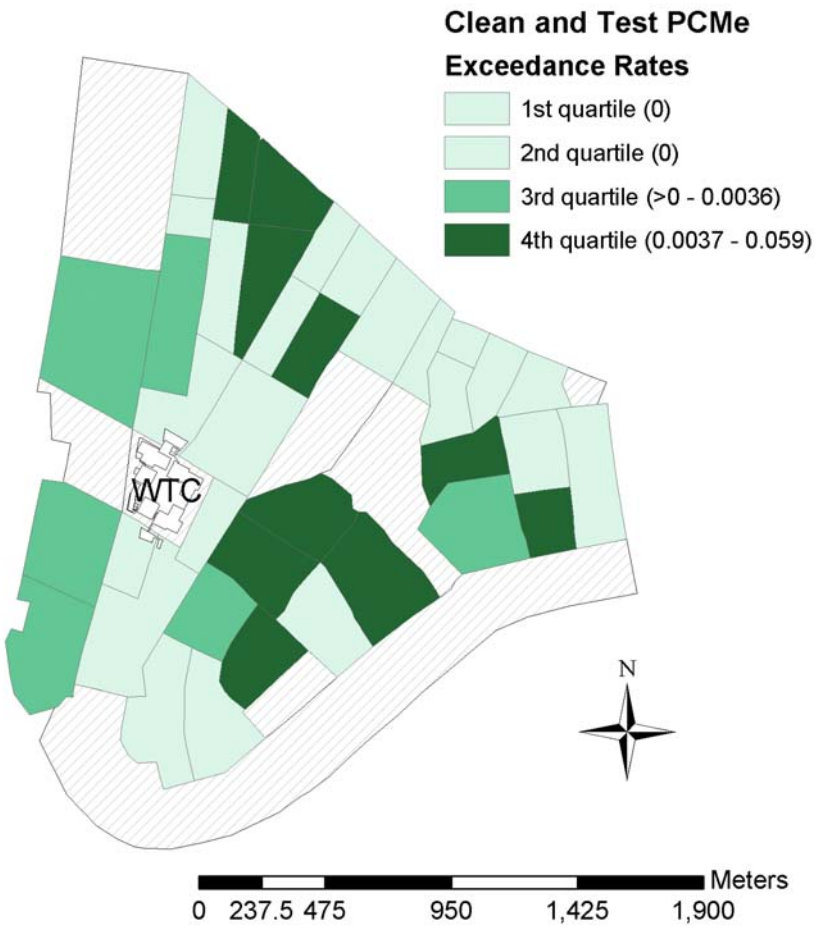

Figure B-14. Spatial distribution of PCMe exceedance rates for the *clean and test* data, by statistical summary areas. *Clean and test* data refers to samples collected from residences where the residents had requested EPA to clean their residences and test their indoor air for asbestos. Quartiles of the distribution of PCMe exceedance rates are shown. Statistical summary areas (SSAs) with one or more exceedances fall in the upper two quartiles, indicating the rareness of the exceedance events. Statistical summary areas with exceedance rates in the upper quartile of the distribution of PCMe exceedances are located north and east of the WTC site. Modest positive spatial autocorrelation in the exceedance rates is indicated by the tendency for SSAs with similar rates to be located near each other.

the PCMe exceedances is made difficult by the low rate of exceedances and the lack of data for some SSAs (discussed further in Appendix D).

Fitting Poisson models to PCMe exceedances

The binomial and Poisson distributions are reasonable statistical models for the PCMe exceedances (Section B.2.1.3). Binomial and Poisson distributions were fit to log-transformed rates[8] for the *test only* and *clean and test data* (second and third columns of Tables B-8 and B-9, respectively). The assumption of equal mean and variance, which is a feature of the Poisson model (Section B.2.1.3), was assessed by fitting a negative binomial model to the data (Appendix D). The estimates of the dispersion parameters for the fitted negative binomial models (Tables B-8 and B-9) indicated that the assumption of equidispersion may be very poor for the *test only* and *clean and test* exceedance rates (i.e., the mean and variance of the rates may not be constant across the SSAs). Violation of the equidispersion assumption has affects similar to violations of the constant variance assumption with a normal distribution model (Cameron and Trivedi, 1998)[9]. A consequence of the violation is a tendency for a loss of power to detect actual differences in PCMe rates between SSAs (Griffith and Layne, 1999). Similarly, failure to consider spatial autocorrelation present in data can lead to a loss of statistical power (Griffith and Layne, 1999).

Very often, remedial measures designed to reduce one type of model violation also reduce the violation of other assumptions. With this in mind, a spatial filter approach was used to account for the spatial autocorrelation present in the data; the approach is described briefly in Appendix D and thoroughly in (Griffith, 2002). Estimates of the parameters for the binomial and Poisson models with the spatial autocorrelation filter added, for the *test only* and *clean and test* data, are shown in the last three columns of Tables B-8 and B-9, respectively. The parameter estimates for

---

[8] The Poisson models were actually fit to log-transformed counts of exceedances, with the log of the number of samples included in the model as an offset variable. This is mathematically equivalent to fitting the Poisson model to the log-transformed rates; see Appendix C for further explanation.

[9] Violation of the constant variance assumption with the normal distribution model affects the significance level (p-values) reported for statistical tests, such as the comparison of the PCMe rates between SSAs. The actual error rates (i.e., type I error rate, α) will tend to be larger than the intended error rate (Griffith and Layne, 1999).

the binomial and Poisson models are very close for both sets of exceedance rates; however, the Poisson model provides

Table B-8. Model Estimation Results for the Log-transformed *Test Only* PCMe Exceedance Rates.

The binomial and Poisson distributions are plausible models for the PCMe exceedances as both distributions can be used to describe count data. A spatial filter derived from the spatial autocorrelation that is expressed by the data was added to both models. Addition of the filter has a substantial impact on the parameter estimates. The apparent violation of the equidispersion assumption (i.e., equal mean and variance) of the Poisson model was rendered inconsequential after the spatial filter was added (see Appendix C for details). The Poisson model is more appealing for the PCMe exceedances due to the rarity of their occurrence and provides a better fit to the data, accounting for approximately twice the variance that is explained by the binomial model.

	Prior to Considering Spatial Autocorrelation[a]		With Spatial Filter Added to Models[a]		
Model	Parameter Estimate	Equi-dispersion	Parameter Estimate	Equi-dispersion	% Variance Accounted for
Binomial	-5.3183	NA	-6.0572	NA	30%
Poisson	-5.3232	NA	-6.0625	NA	60%
Negative binomial[b]	-5.0964	4.6066	-6.1506	0.4476	

[a]Spatial autocorrelation is accounted for in the statistical models using an eigenfunction spatial filter (Griffith, 2002); see Appendix B for details.
[b]A negative binomial distribution was fit to the PCMe exceedances to assess the assumption of equidispersion (equal mean and variance), which is a feature of a Poisson random variable.

Table B-9. Model Estimation Results for the Log-transformed *Clean and Test* PCMe Exceedance Rates.

The binomial and Poisson distributions are plausible models for the PCMe exceedances as both distributions can be used to describe count data. A spatial filter derived from the spatial autocorrelation that is expressed by the data was added to both models. The apparent violation of the equidispersion assumption (i.e., equal mean and variance) of the Poisson model was reduced by the addition of the spatial filter to the model (see Appendix C for details). The Poisson model is more appealing for the PCMe exceedances due to the rarity of their occurrence; both models explain approximately the same percent of the variance in the data.

	Prior to Considering Spatial Autocorrelation[a]		With Spatial Filter Added to Models[a]		
Model	Parameter Estimate	Equi-dispersion	Parameter Estimate	Equi-dispersion	% Variance Accounted for
Binomial	-5.4713	NA	-5.9347	NA	40%
Poisson for rates	-5.4756	NA	-5.9383	NA	40%
Negative binomial[b] for rates	-5.2098	2.8692	-[c]		

[a]Spatial autocorrelation is accounted for in the statistical models using an eigenfunction spatial filter (Griffith, 2002); see Appendix B for details.
[b]A negative binomial distribution was fit to the PCMe exceedances to assess the assumption of equidispersion (equal mean and variance), which is a feature of a Poisson random variable.
[c]The negative binomial not estimable; however, the deviance measure for the Poisson model (1.38) indicates overdipsersion has been reduced.

a much better fit for the *test only* exceedance rates; the fit is approximately the same for the *clean and test* exceedance rates.

Five buildings accounted for 6,470 (27%) of the *clean and test* sample results. A subset of the *clean and test* data was created by removing these 6,470 measurements from the database. The binomial and Poisson models were refit to the data to assess the effect of these five buildings on the estimates of the model parameters, and their effect on the goodness-of-fit of the models to the data. The parameter estimates differed slightly, and both models continued to account for approximately 40% of the variance in the data. Based on these results, the spatial autocorrelation-filtered Poisson models with parameters -5.94 and -6.06 (log-transformed rates of exceedances) were used to describe the *clean and test* and *test only* data, respectively.

Comparison of PCMe Exceedance Rates

Exceedance rates for each SSA with a sample size of 30 or more were compared to each other to assess whether or not statistically significant differences exist. Aggregate sample sizes less than 30 were considered too small to include in the comparisons. The sample size restriction left 22 SSAs for the *test only* data and 32 for the *clean and test* data. Comparisons were based on the spatial autocorrelation-filtered Poisson models described above. These comparisons essentially consist of calculating the difference between the rates for two SSAs, and determining if the absolute value of the difference is statistically different from zero. In general, the differences in the exceedance rates will approach a normal distribution as the means for the rates increases. The normal approximation is very good when the number of exceedance for each SSA exceeds 4. The low number of exceedances in most SSAs indicated the normal approximation would be poor. This was confirmed by a simulation experiment which showed that the normal distribution would not be reasonable for either the *test only* or *clean and test* exceedance rates comparisons. Therefore, the significance of each of the pairwise comparisons between SSA exceedance rates was determined by nonparametric simulation analysis. The simulation experiments are described in Appendix D.

Pairwise comparisons that were significant at type I error rates (α) of 0.01, 0.05 and 0.10 are shown in Appendix D, Tables D-1 and D-2. The type I error rates reported are global error rates that take into consideration the multiple comparisons that are being made. When performing multiple statistical tests, the probability of rejecting the null hypothesis when it is true (Type I

error, α) increases. In the present context, this means the probability of incorrectly concluding that a difference exists between the exceedance rates for two SSAs would be greater than intended, unless the error rate was adjusted to compensate for the multiple tests. The error rates reported in Tables D-1 and D-2 reflect a Bonferroni adjustment to account for the multiple tests (see Appendix D for details).

The comparisons of the *test only* exceedance rates between SSAs indicate there are three SSAs with exceedance rates that are statistically significantly different (at $\alpha = 0.01$) than the exceedance rates observed in approximately one-half of the other SSAs (Figure B-15a)

Results of the comparison of the *clean and test* exceedance rates between SSAs are indicated in Figure B-15b. The number of significant pairwise comparisons at $\alpha = 0.01$ are shown for SSAs that had one or more exceedance. Three SSAs that differ from the majority of the other SSAs are located east of the WTC. The number of exceedances for these three SSAs range from 17 – 32; the exceedance rates range from 0.006 to 0.059.

The SSA-level analysis has shown that the Poisson model provides a reasonable model for the PCMe exceedance rates after the model is modified to account for the positive spatial autocorrelation that is exhibited by the exceedance rates. The comparisons of the exceedance rates indicate that the rates are not constant across the SSAs. Statistical summary areas having the highest rate of PCMe exceedances are located east of the WTC site.

B.3.2.3 Building-Level Pattern of PCMe Exceedance

Two methods for testing for the presence of clusters in the exceedance events, Nearest Neighbor distances and Ripley K functions, are briefly described in this section. Both methods can be used to produce plots of the spatial distribution of sample locations, and the spatial distribution of PCMe exceedance locations. Visual comparison of these plots can provide useful qualitative information regarding the presence or absence of spatial clustering of the PCMe exceedance events. A formal statistical test for spatial randomness is available for the nearest neighbor distance. A semi-quantitative, graphical method is used with the Ripley K function to test for spatial randomness. The underlying assumption behind both

methods, as they are employed in this analysis, is that PCMe exceedances follow a homogeneous spatial Poisson process as described in Section B.2.1.3.

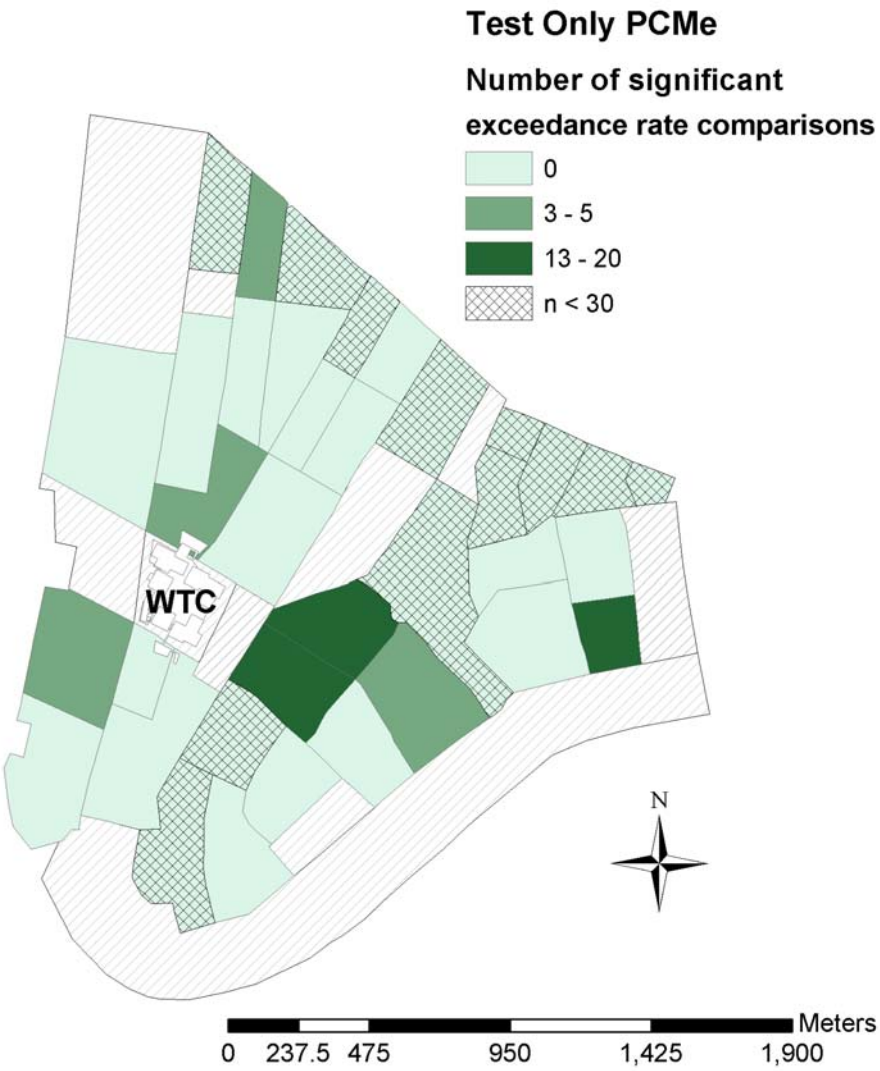

Figure B-15a. Significant differences between estimated exceedance rates for *test only* data. Estimates are based on the spatially-filtered Poisson model (see Section 3.2.3.2 and Appendix D for details). The number of significant pairwise comparisons at an experiment-wise $\alpha = 0.01$ (with a Bonferroni adjustment) are shown for SSAs that had one or more exceedances. Comparisons with SSAs with sample sizes less than 30 (indicated in figure by cross-hatching, and in figure legend by "n<30") were deemed unreliable and were therefore not included in the analysis. The 3 SSAs that were found to have the most number of significant comparisons are located east of the WTC. The numbers of exceedances for these three SSAs range from 2 to 9; their exceedance rates range from 0.021 to 0.060. The spatial pattern exhibited above is similar to the pattern of exceedance rates that is shown in Figure 3-13 however, 4 of the 7 SSAs with exceedance rates in the 4^{th} quartile (Figure 3-13) were found to be significantly different from 5 or fewer of the other SSAs.

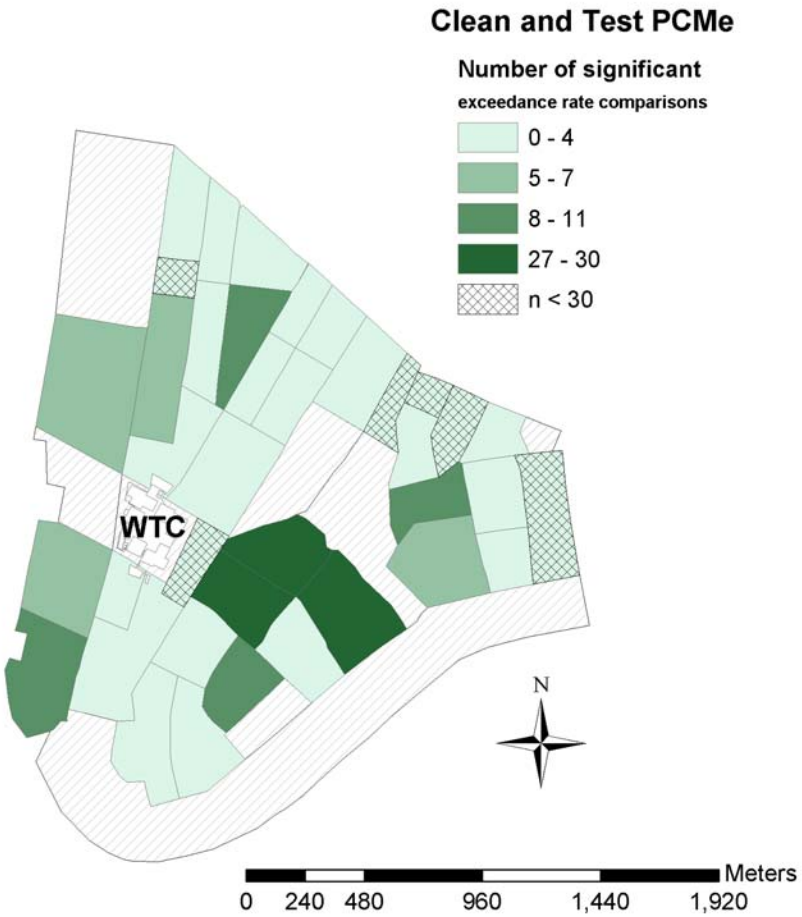

Figure B-15b. Significant differences between estimated exceedance rates for *clean and test* data. Estimates are based on the spatially-filtered Poisson model (see Section 3.2.3.2 and Appendix D for details). The number of significant pairwise comparisons at an experiment-wise $\alpha = 0.01$ (with a Bonferroni adjustment) are shown for SSAs that had one or more exceedances. Comparisons with SSAs with sample sizes less than 30 (indicated in figure by cross-hatching, and in figure legend by "n<30") were deemed unreliable and were therefore not included in the analysis. Three of the SSAs that were found to have the most number of significant comparisons are located east of the WTC. The numbers of exceedances for these three SSAs range from 17 to 32; their exceedance rates range from 0.006 to 0.059. The spatial pattern exhibited above is similar to the pattern of exceedance rates that is shown in Figure 3-14 however, 3 of the 9 SSAs with exceedance rates in the 4th quartile (Figure 3-14) were found to be significantly different from 4 or fewer of the other SSAs.

The location of the *test only* and *clean and test* buildings are not evenly distributed across the potentially affected area. For example, the buildings can be grouped into five sub areas. The largest dimension of these areas varies from approximately 750–1,500 meters. Therefore interpretation of these analyses should be limited to distances of 500–750 meters, as distances greater than these may be overly influenced by global trends in the events, rather than the local spatial dependence between events.

Nearest Neighbor Method

In nearest neighbor analysis, the focus is on the distance between the exceedance events. The observed nearest neighbor distance $\overline{NNd}$ is the average distance between each exceedance events and its closest neighbor (i.e., another exceedance event). It is calculated by determining the distance between each event and its nearest neighbor, then taking the average of the distances. The observed $\overline{NNd}$ is compared to the average distance between nearest neighbors that would be expected if the events were randomly distributed in space (i.e., if they followed a spatial Poisson process). The expected distance is provided by:

$$E(NNd) = \frac{1}{2\sqrt{\hat{\lambda}}}; \qquad \hat{\lambda} = N / A \qquad \text{Equation B-5}$$

where, E(NNd)=expected average distance between nearest neighbors, under the assumption that the events follow a spatial Poisson process; λ=mean, or intensity, of the spatial Poisson process, which is estimated by the total number of events (N), divided by the area of the site (A). The ratio of the observed nearest neighbor distance to the expected nearest neighbor distance yields the nearest neighbor index (NNI):

$$NNI = \left(\overline{NNd}\right) / E\left[NNd\right] \qquad \text{Equation B-6}$$

Nearest neighbor indexes equal to one indicate complete spatial randomness (CSR; i.e., homogeneous Poisson process); NNIs less than one indicate spatial clustering, and NNIs greater than one indicate dispersion, or regular spacing (e.g., a square grid).

An important concern in this analysis is how much lower (greater) than one does the NNI have to be to conclude the events are clustered (dispersed). A test for the significance of NNI (i.e., lack of clustering or dispersion in the location of PCMe exceedances) may be performed by computing the standardized estimate of the NNd (Z) (Equation B-7) and then comparing the calculated Z to a table of the standard normal distribution (Clark and Evans, 1954):

$$Z = \frac{\overline{NNd} - E[NNd]}{SE_{\overline{NNd}}} \qquad \text{Equation B-7}$$

Where $SE_{\overline{NNd}}$ =standard error of the estimate of the mean nearest neighbor distance:

$$\mathrm{SE}_{\overline{\mathrm{NNd}}} = \sqrt{\frac{(4-\pi)}{4\pi \mathrm{N}}} \qquad \text{Equation B-8}$$

A shortcoming of the above test is that it assumes the data are a random sample from the population (Bailey and Gatrell, 1995; Dixon, 2001), which has already been determined to be invalid for the PCMe data. A second shortcoming of the test is that it ignores the correlation between nearest neighbor distances (Cressie, 1993; Dixon, 2001). An extreme case of the correlation is two exceedance events that are the nearest neighbor of each other (i.e., *reflexive nearest neighbors*). Under the assumption of complete spatial randomness (CSR) in two dimensions, approximately 62% of the events of a spatial point pattern are reflexive nearest neighbors (Dixon, 2001). Finally, nearest neighbor analysis assumes that exceedance events are from a continuous, isotropic surface. The geographic distribution of the sampled buildings represent a distribution of discrete objects rather than a continuous surface, and it is not equal in all directions (i.e., the distribution is anisotropic).

Given the shortcomings of the above approach, a numerical simulation approach was used to test the significance of the NNd. The simulation approach generates a list of possible ways of assigning *N* exceedance 'labels' to *B* buildings, where *N* equals the number of exceedance events (i.e., *N*=8 for *test only* and 37 for *clean and test* data) and *B* equals the number of sampled buildings (i.e., *B*=219 for *test only* and 408 for *clean and test* data). The observed pattern of exceedance events is then compared to the list of possible patterns to test the hypothesis that the exceedance events are randomly distributed geographically (the average NNd for the observed

pattern of events is compared to the ranked list of NNDs for the simulated values). If the observed NNd is typical of the simulated values, the null hypothesis of first order spatial randomness is not rejected; if the observed value is smaller or larger than most of the simulation NNds, the null hypothesis is rejected.

Another advantage of the simulation test is it removes the assumption that the exceedance events follow a random spatial Poisson process. The simulation test detects departures from spatial randomness, rather than departures from a specific type of random process.

The numerical simulation was executed by randomly selecting *N* buildings (without replacement) from the list of *B* buildings that were sampled for PCMe. The NNd was then calculated for the *N* randomly selected buildings and saved. This process was repeated 9,999 times, producing 9,999 NNds. The NNd that was calculated for the actual data was then added to the list of 9,999 simulated values. The 10,000 NNds were then ranked from lowest to highest. A two-sided test of the null hypothesis that the exceedance events are consistent with a first order spatial random process can be made by comparing the rank of the observed NNd divided by 10,000 to (1–α/2), where α is the chosen level of significance, and rejecting the null hypothesis if the simulated p-value is greater than (1–α/2).

In addition to calculating a NNI for the distances between the closest nearest neighbors (i.e., first order nearest neighbors), it is often informative to calculate NNIs for second, third, …, K-th nearest neighbors. For example, the k=2 (*second order*) NNI is the ratio of the average distance between each PCMe exceedance and its second nearest neighbor $\left(\overline{NND}\right)_{k=2}$, and the expected NND for k=2 $\left(E\left[NNd\right]_{k=2}\right)$:

$$\left(E\left[NNd\right]_{k=2}\right)=\frac{K(2K)!}{(2^K K!)^2\sqrt{N/A}} \qquad \text{Equation B-9}$$

Evaluating the average nearest neighbor distance at orders greater than one provides a description of the interaction between events at increasing separation distances. Equations B-8 and B-9 are appropriate for first order NNds; significance tests for higher order NNds have not been developed.

The NNIs for the exceedance events should be compared to the NNIs for the sampled buildings to account for the nonrandom sampling methods that were employed. A relative NNI is calculated as the ratio between the NNI for the exceedance events and the NNI for the sampled buildings. Relative NNIs less than (greater than) one indicate clustering (dispersion) of events that is not explained by the spatial distribution of the sampled buildings. The relative NNI is a qualitative measure; statistical tests for significance are not available.

Nearest Neighbor Results

The simulation test for the significance of the *test only* NNd failed to reject the null hypothesis of first order spatial randomness, although the small number of exceedances (8) should be considered. The simulation test for the *clean and test* exceedance events also failed to reject the null hypothesis of first order spatial randomness (p=0.33). The p-value indicates that 33% of the simulated patterns of *clean and test* exceedance events had NNds smaller than the observed NNd. These results argue against significant spatial clustering of the PCMe exceedances at the site (i.e., more than would be expected by chance).

Table B-10 shows the NNI and relative NNI for the first 5 'orders' of neighbors. The table indicates that the *test only* events are more dispersed than the *test only* buildings. These results should be interpreted with caution due to the small number of *test only* exceedance events (8). The *clean and test* exceedance events exhibit clustering that is consistent with the clustering observed in the sampled buildings. Figure B-16 shows the NNI for the first 20 orders of neighbors. The *test only* and *clean and test* events plot above the sampled buildings, indicating that the events are not clustered. At higher orders of neighbors, the *clean and test* events are slightly more dispersed relative to the spatial distribution of sampled buildings. The results for higher orders also should be interpreted with caution due to the low number of exceedances (37). Overall, results from the nearest neighbor method lead to a rejection of the null hypothesis that the exceedance events are clustered.

Ripley's K Function

Ripley's K function (K function) is another method for assessing whether the exceedance events are clustered. While the NNd looks at the distance between nearest events at increasing orders, the K function looks at the number of neighbors at increasing distances. The number of

neighbors is determined by drawing a circle of radius *r* around each event and counting the number of other events ('neighbors') that fall within the circle (Figure B-17). This is repeated for every event. Ripley's K function for distance *r* equals the total number of neighbors that were counted over all the events:

$$K(r) = \frac{A}{N^2} \sum_{i=1}^{N} \sum_{j=1}^{N} I(d_{ij}) \qquad \text{Equation B-10}$$

Table B-10. Nearest Neighbor Statistics for the PCMe Exceedances.

The nearest neighbor distance (NNd) for *order 1* is the average distance between the location of each PCMe exceedance and its nearest neighbor. Second order NNds correspond to the average distance between the location of each PCMe exceedance and its second nearest neighbor, etc. Nearest neighbor indexes (NNIs) equal the NNd divided by E[NNd]. NNIs less than (greater than) 1 indicate spatial clustering (dispersion) of PCMe exceedances. The NNIs for the spatial distribution of sampled buildings indicate the buildings tend to be clustered, which is typical for the geographical distribution of buildings in an urban environment. Proper interpretation of the NNIs for the exceedances requires comparing the nearest neighbor indexes (NNIs) for the exceedances to the NNI for the sampled buildings. The relative NNIs for the *clean and test* and *test only* PCMe exceedances indicate a lack of spatial clustering (i.e., they are greater than 1). The results shown are approximate; the E[NNd] assumes the PCMe data were gathered using random sampling methods, or the that the entire population was measured; neither assumption is valid given the data were obtained by voluntary participation in the WTC dust cleanup program.

***Test Only* Buildings**				***Test Only* Exceedances**			
Order	NNd[a]	E[NNd][b]	NNI[c]	NNd[a]	E[NNd][b]	NNI[c]	Rel-NNI[d]
1	50.87	62.10	0.82	406.42	324.91	1.25	1.53
2	73.80	93.15	0.79	725.19	487.37	1.49	1.88
3	91.54	116.44	0.79	910.49	609.21	1.49	1.90
4	110.03	135.84	0.81	1071.27	710.74	1.51	1.86
5	124.26	152.82	0.81	1253.63	799.59	1.57	1.93
***Clean and Test* Buildings**				***Clean and Test* Exceedances**			
Order	NNd[a]	E[NNd][b]	NNI[c]	NNd[a]	E[NNd][b]	NNI[c]	Rel-NNI[d]
1	33.74	45.50	0.74	118.45	151.08	0.78	1.06
2	52.59	68.24	0.77	170.72	226.62	0.75	0.98
3	65.61	85.31	0.77	224.41	283.28	0.79	1.03
4	76.22	99.52	0.77	278.31	330.49	0.84	1.10
5	85.79	111.96	0.77	326.16	371.80	0.88	1.14

[a]NNd: nearest neighbor distance (meters)
[b]E[NNd]: expected nearest neighbor distance, under assumption of complete spatial randomness (CSR)
[c]NNI: nearest neighbor index
[d]Rel-NNI: relative nearest neighbor index=NNI for exceedances/NNI for all buildings

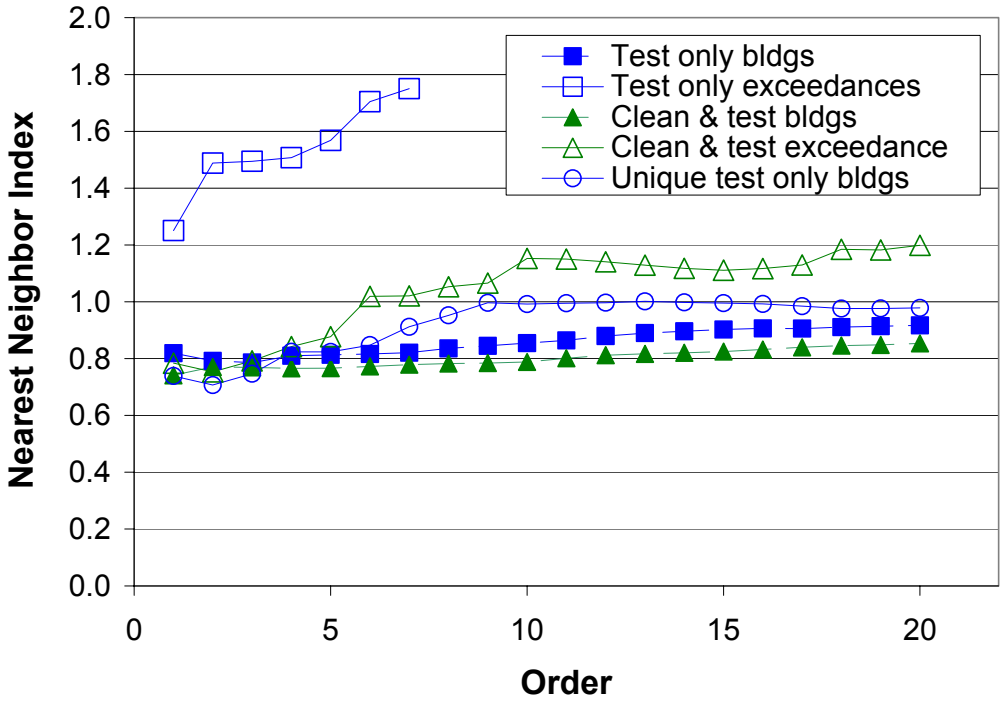

Figure B-16. Nearest neighbor analysis for the PCMe asbestos data. The nearest neighbor index (NNI) is the ratio of the observed nearest neighbor distance (NNd; average distance between each PCMe exceedance and its closest neighbor) to the expected value of the NNd, under the assumption of complete spatial randomness (CSR). A NNI of 1 indicates a random spatial distribution of events; NNIs < 1 indicate clustering, NNIs >1 indicate dispersion (e.g., spatial distribution of PCMe exceedances on a square grid). The x-axis of the figure indicates the average distance between neighbors of increasing *orders*; e.g., the NNI of *order =2* is the ratio of the average distance between each PCMe exceedance and its *second* closest neighbor, and the expected distance between neighbors of order = 2. The NNIs for the building locations indicate spatial clustering at small spatial scales (i.e., low *orders*). The buildings approach a random distribution (i.e., NNI = 1) at larger spatial scales (i.e., higher orders). This pattern is typical of the geographic distribution of buildings in an urban landscape. The NNIs for the clean and test exceedances are very similar to the NNIs for the clean and test buildings;, up to order =5, indicating a lack of spatial clustering of the exceedances, relative to the building locations; clean and test exceedances events appear to be randomly distributed among the sampled clean and test building locations. At orders greater than 5, the clean and test exceedance events appear to be spaced further apart on average than expected for a random distribution. However, given the small number of clean and test exceedances (37), the NNIs at higher orders should be interpreted with caution. The test only exceedance events appear to dispersed; however the very low number of test only exceedance events (8) preclude drawing definitive conclusions. All of the *test only* exceedances occurred in buildings that also contained at least one residence that was also cleaned and tested. Furthermore, the analysis of spatial trends (further discussed in Section 3.2 of the report) indicate that buildings with only *test only* residences (*unique test only*) tend to be located north of the buildings that also contained *clean and test* residences. This difference between the spatial distribution of the *test only* and *unique test only* buildings probably contributes to the dispersion indicated by the NNI for the *test only* exceedance events.

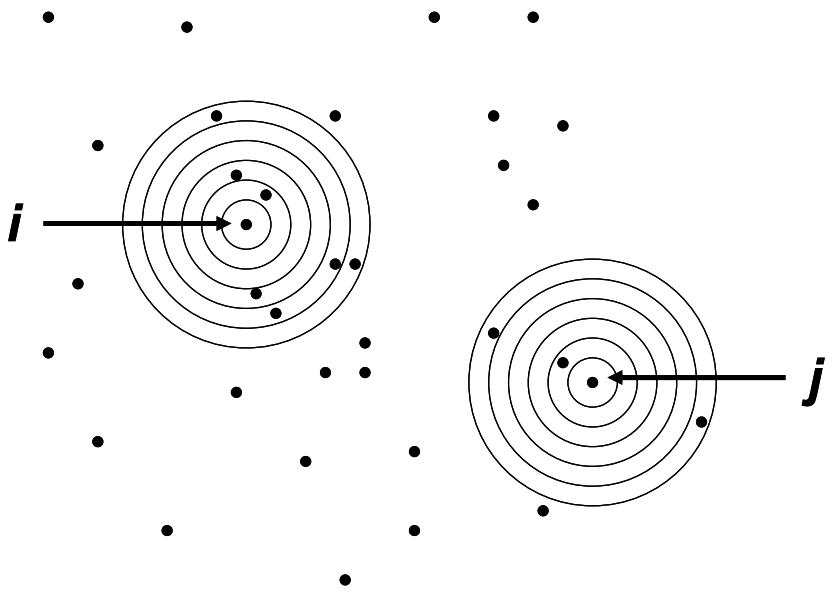

Figure B-17. Calculation of the Ripley K function. The Ripley K function is estimated by counting the number of other exceedance events that are located within a distance *r* of an exceedance event. The calculation is repeated for every event, *i*, *j*, ….*N*, where *N* = the number of events. The Ripley K function for separation distance r is the sum of all counts over all events (Equation 6, Section 3.2.2.2.3). Ripley's K function is typically repeated for increasing separation distances and plotted vs the separation distances (e.g., Figures 3-11, 3-12). Shown above is the calculation for two events, *i* and *j*, for six separation distances (corresponding to the six circles). The concentric circles represent increasing separation distances (*r*). For example, Event *i*: 0 other events (i.e., other exceedances) within distance of 1 unit, 7 other events within a distance of 6 units; event *j:* 1 other event within a distance of 3 units, and 3 other events within a distance of 6 units.

Where, r=radius of circle that is used to define neighbors, A=area of site, N=number of exceedance events, d_{ij}=distance between points i and j, I=indicator variable that=1 if $dij < r$ and 0 otherwise.

This calculation is repeated, each time increasing the radius r of the circle that is used to define *neighbors*, up to the desired maximum value of r.

Interpretation of the K function is typically performed by plotting a conversion of K(r), L(r), versus r:

$$L(r) = \sqrt{\frac{K(r)}{\pi}} - r \qquad \text{Equation B-11}$$

The conversion to L(r) is made to make the plot easier to interpret. Values of L(r) greater than 0 indicate clustering; values less than 0 indicate dispersion.

Under the assumption that the exceedance events are distributed according to a random spatial Poisson process, the expected number of events within distance r of a given event is:

$$E[K(r)] = \frac{N}{A}\pi r^2 \qquad \text{Equation B-12}$$

where, N=number of events, A=area of site, and r=radius of circle that is used to define neighbors.

The expected value of the K-function, after conversion to L(r) (Equation B-11), plots as a horizontal line at L(d)=0. If the number of other exceedance events found within a distance r from an exceedance event is greater than E(K[r]), clustering is indicated at that distance; conversely, if the number of events at r is less than the expected value, dispersion is indicated.

The weighted Ripley's K function was estimated for the two groups of exceedance events, where the events are weighted by the number of samples that were collected from each building. The weights account for the increased likelihood of measuring an exceedance in buildings where more samples are collected (Levine, 2002).

The sampling distribution of K(r) has not been determined. Therefore, a test for CSR was performed using a simulation approach that is similar to the one that was used to test the significance of the NNI. The numerical simulation was executed by randomly selecting *N* buildings (without replacement) from the list of *B* buildings that were sampled for PCMe. The values of L(r) were then calculated for the *N* randomly selected buildings for different values of *r* and saved. This process was repeated 9,999 times, producing 9,999 estimates of L(r) at each distance, *r*. *Simulation envelopes* were created by plotting extreme values of the simulated L(r) at each distance. The significance of the estimated K-function at each distance *r* was made by comparing it to the s*imulation envelopes*.

Ripley's K Function Results

Figures B-18 and B-19 show the K-function for the *test only* and *clean and test* events plot below the *test only* and *clean and test* buildings, respectively, which indicates that the exceedance events are more dispersed than the geographic distribution of the sampled buildings. The exceedances also appear to be dispersed relative to the location of the sampled buildings, after the Ripley K function is adjusted to consider the number of samples that were collected from each building. At separation distances greater than approximately 400 feet, the curve for the exceedances falls at or below the curve that corresponds to the 5th percentile of the simulated Ripley K values, indicating that the pattern of *test only* exceedances may be more dispersed than expected based on chance alone for a spatially random process. However, given the small sample number of exceedances (*n*=8), these results should be interpreted with caution.

The Ripley K function for the *clean and test* exceedances indicates that the exceedances are slightly dispersed relative to the location of the sampled buildings. Some slight clustering of exceedance events may be indicated at the smallest separation distance considered (i.e., approximately 100 meters) when the exceedances are compared to the Ripley K function for the sampled buildings after it is adjusted to consider the number of samples that were collected from each building. However, the curve for exceedance events falls between the 5th and 95th percentile of the simulated Ripley K values, indicating that the pattern of exceedances does not differ significantly from a spatially random process. Overall, the analyses provide no convincing evidence of clustering in either the *clean and test* or *test only* exceedance events.

B.3.2.4 Site-Level Vertical Pattern of PCMe Exceedance

Analysis of the vertical pattern of PCMe exceedances was performed using contingency tables and by fitting Poisson regression models to the data. Floor levels were used as a surrogate for elevation. Early

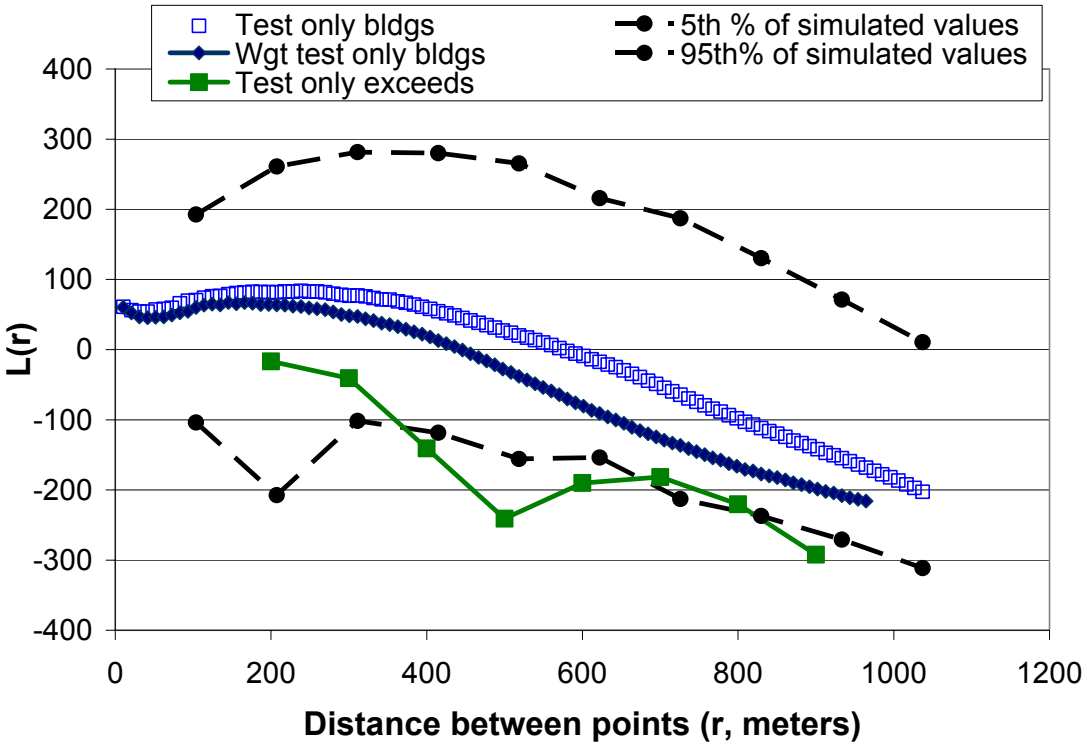

Figure B-18. Ripley's K plot for the *test only* PCMe exceedance event data. A Ripley's K plot is used to compare the number of neighbors for each exceedance event (i.e., location of building with at least one PCMe results > 0.0009 f/cc) to an expected number of neighbors based upon the null hypothesis that the events are randomly distributed across the geographic landscape according to a homogenous spatial Poisson process (see Section 3.2.1.3 for explanation). The number of neighbors is determined by drawing a circle of radius *'r'* around each event and counting the number of other events ('neighbors') that fall within the circle. This is repeated for every event. Ripley's K function for radius 'r' equals the total number of neighbors that were counted over all the events. This calculation is repeated, each time increasing the size of the circle that is used to define *neighbors*; the increasing radius is shown on the x-axis. A conversion of K(r) to L(r) (see Section 3.2.2.2.3 for definition) is made to make the plot more linear (i.e., easier to interpret). Values of L(d) greater than 0 indicate clustering; values less than 0 indicate dispersion. Ripley's K for the *test only* PCMe events is consistent with the nearest neighbor plot (Figure 3-7); the geographical distribution of the *test only* events exhibit less clustering than the *test only* buildings, respectively. A weighted Ripley's K function was estimated for the sampled buildings, where the events are weighted by the number of samples that were collected from each building. The weights account for the increased likelihood of measuring an exceedance in buildings where more samples are collected. A comparison of the Ripley K function for the *test only* events to the weighted Ripley K indicates that the exceedances are dispersed relative to the sampled buildings. The location of the Ripley K plot for the exceedances within the simulation envelope (see Section 3.2.2.2.3 for details), which is defined by the 5th and 95th percentile of the simulated Ripley K function at each distance interval (*r*), supports a conclusion that there is insufficient evidence to indicate clustering of the test only exceedance events.

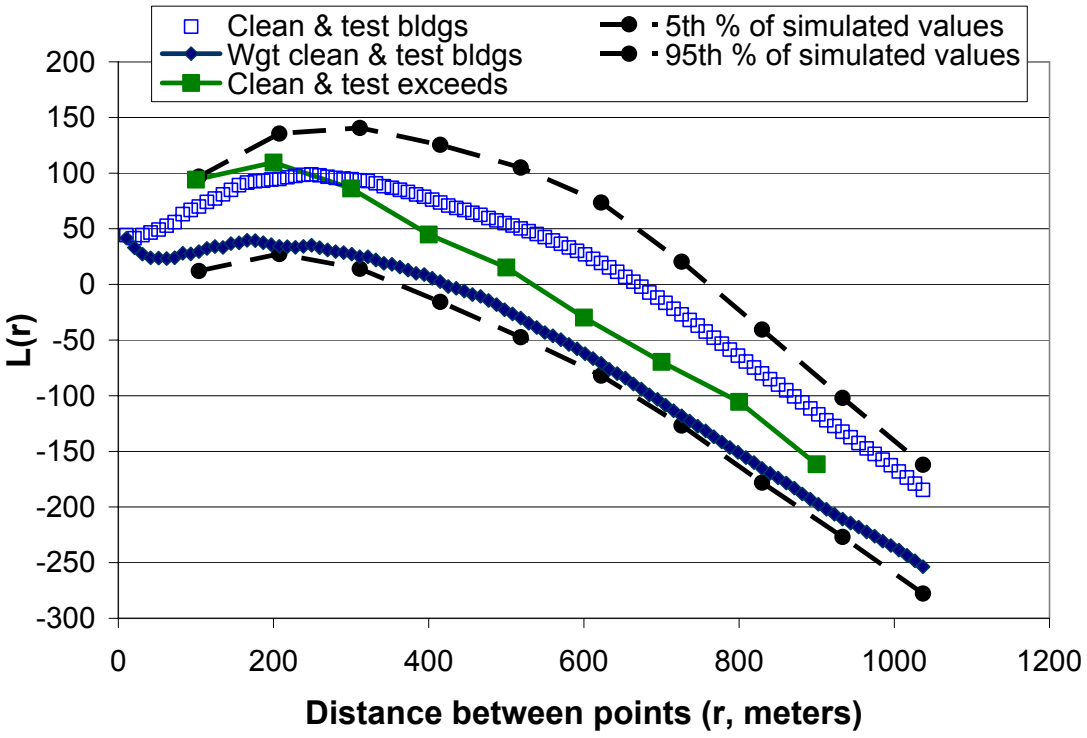

Figure B-19. Ripley's K plot for the *clean and test* PCMe exceedance event data. The Ripley's K plot for the *clean and test* PCMe events is consistent with the nearest neighbor plot (Figure 3-7); the geographical distribution of the *clean and test* events exhibit less clustering than the *clean and test* buildings. A comparison of the Ripley K function for the *clean and test* events to the weighted Ripley K function indicates that the exceedance events appear to be slightly more clustered than the sampled buildings, particularly at short distances. The location of the Ripley K plot for the exceedances within the simulation envelope (see Section 3.2.2.2.3 for details), which is defined by the 5th and 95th percentile of the simulated Ripley K function at each distance interval (*r*), fails to support a conclusion that the exceedance events are clustered.

attempts at fitting a Poisson model using individual floor levels were unsuccessful due to the rarity of exceedances. To address this problem, floors were grouped into three categories: lower floors (floors 3 and lower), middle floors (floors between 4 and 9, inclusive), and upper floors (floors 10 and higher). The analysis was performed in two ways. The first approach was performed at the sample level (*sample-basis*); each sample result was used in the analyses (i.e., the exceedance events were *not* aggregated at the building level). In the second approach (*residence-basis*), the data were aggregated at the residence level; any residence that had one or more exceedance was treated as an exceedance.

Sample-Basis Analysis

Contingency tables for the *test only* and *clean and test* data are provided as Tables B-11 and B-12.

All of the exceedance rates are less than 1%. Fisher's exact test for the *test only* data indicates the difference in exceedance rates between floors is marginally significant (p=0.08, 2-sided). A higher exceedance rate was observed for the middle floor group (0.73%) then either the lower (0.11%) and upper (0.37%) floor groups. Additional tests were performed between the floor groups to determine which exceedance rates were significantly different, if any. The difference between the *lower* floor group and the *middle* floor group was found to be significant by Fisher's exact test (p=0.04, 2-sided); differences between the middle and upper, and lower and upper floor groups were not statistically significant by Fisher's exact test (p=0.17 and p=0.43, respectively; 2-sided). The Poisson model for the *test only* data was not significant.

Fisher's exact test for the *clean and test* data indicates the difference in exceedance rates between floors is statistically significant (p=0.02, 2-sided). The exceedance rate was highest for the lower floor group (0.66%), lower for the middle floor group (0.44%), and the lowest for the upper floor group (0.32%). Additional tests were performed between the floor groups to determine which exceedance rates were significantly different. The difference between the lower and upper floor groups was found to be statistically significant by Fisher's exact test (p=0.01; 2-sided). The differences between the *lower* and *middle* floor group, and the *middle* and *upper* floor group were found to be not significant by Fisher's exact test (p=0.12, p=0.20, respectively; 2-sided). The odds ratios for the Poisson model indicate lower floors are twice as likely to have exceedances as the upper floors (95% CI 1.2, 3.4) (p-value for chi-square test for parameter = 0.01).

Table B-11. Contingency table for *test only* PCMe exceedances, on a sample-basis.			
The exceedance rate in the middle floor group is higher than the exceedance rates observed in the lower and upper floor groups. The p-value for Fisher's exact test is 0.08, indicating the differences between the floor groups is marginally statistically significant.			
Floor Group	Not PCMe exceedances	PCMe exceedances	Totals
lower	873[a] 99.89[b]	1[c] 0.11[d]	874
middle	1768 99.27	13 0.73	1781
upper	1617 99.63	6 0.37	1623
Totals	4258 99.53	20 0.47[e]	4278[e]

[a]Number of samples that did not exceed health-based benchmark for asbestos
[b] Percent of samples that did not exceed health-based benchmark for asbestos
[c]Number of samples that exceeded the health-based benchmark for asbestos
[b] Percent of samples that exceeded the health-based benchmark for asbestos
[e] The table does not include samples where the floor was not provided in the database, therefore sample sizes and percent of exceedances will differ from those provided elsewhere in the report.
[e] The table does not include samples where the floor was not provided in the database, therefore sample sizes and percent of exceedances will differ from those provided elsewhere in the report.

Table B-12. Contingency table for *clean and test* PCMe exceedances, on a sample-basis.

The observed exceedance rate increases with floor level. The p-value for Fisher's exact test is 0.02, indicating the differences between the floor groups is statistically significant at the 0.05 level.

Floor Group	Not PCMe exceedances	PCMe exceedances	Totals
lower	4233[a] 99.34[b]	28[c] 0.66[d]	4261
middle	8971 99.56	40 0.44	9011
upper	10488 99.68	34 0.32	10522
Totals	23692 99.57	102 0.43[e]	23794[e]

[a]Number of samples that did not exceed health-based benchmark for asbestos
[b] Percent of samples that did not exceed health-based benchmark for asbestos
[c]Number of samples that exceeded the health-based benchmark for asbestos
[b] Percent of samples that exceeded the health-based benchmark for asbestos
[e] The table does not include samples where the floor was not provided in the database, therefore sample sizes and percent of exceedances will differ from those provided elsewhere in the report.

Residence-Basis Analysis

Contingency tables for the *test only* and *clean and test* data are provided as Tables B-13 and B-14.

Fisher's exact test indicates the exceedance rates do not differ significantly between floor groups for the *test only* and *clean and test* data (p=0.74 and 0.84, respectively), when the data are analyzed at the residence level.

Table B-13. Contingency table for *test only* PCMe exceedances, on a residence-basis.

The exceedances are extremely rare across the floor groups. The p-value for Fisher's exact test is 0.74, indicating the differences between the floor groups is not statistically significant.

Floor Group	Not PCMe exceedances	PCMe exceedances	Totals
lower	147[a] 100[b]	0[c] 0[d]	147
middle	303 99.02	3 0.98	306
upper	292 99.32	2 0.68	294
Totals	742 99.33	5 0.67[e]	747[e]

[a]Number of samples that did not exceed health-based benchmark for asbestos
[b] Percent of samples that did not exceed health-based benchmark for asbestos
[c]Number of samples that exceeded the health-based benchmark for asbestos
[b] Percent of samples that exceeded the health-based benchmark for asbestos
[e] The table does not include samples where the floor was not provided in the database, therefore sample sizes and percent of exceedances will differ from those provided elsewhere in the report.

Table B-14. Contingency table for *clean and test* PCMe exceedances, on a residence-basis.			
Very little difference in the exceedance rate is observed between floor groups. The p-value for Fisher's exact test is 0.84, indicating the differences between the floor groups is statistically significant.			
Floor Group	Not PCMe exceedances	PCMe exceedances	Totals
lower	534[a] 99.07[b]	5[c] 0.93[d]	539
middle	1306 99.24	10 0.76	1316
upper	1497 99.27	11 0.73	1508
Totals	3337 99.23	26 0.77[e]	3363[e]

[a]Number of samples that did not exceed health-based benchmark for asbestos
[b] Percent of samples that did not exceed health-based benchmark for asbestos
[c]Number of samples that exceeded the health-based benchmark for asbestos
[b] Percent of samples that exceeded the health-based benchmark for asbestos
[e] The table does not include samples where the floor was not provided in the database, or common areas, therefore sample sizes and percent of exceedances will differ from those provided elsewhere in the report.